Retrieving aerosol microphysical properties by Lidar-Radiometer Inversion Code (LIRIC) for different aerosol types

M. J. Granados-Muñoz, J. L. Guerrero-Rascado, J. A. Bravo-Aranda, F. Navas-Guzmán, A. Valenzuela, H. Lyamani, A. Chaikovsky, U. Wandinger, A. Ansmann, O. Dubovik, et al.

AGU PUBLICATIONS

JGR

Journal of Geophysical Research: Atmospheres

RESEARCH ARTICLE
10.1002/2013JD021116

Key Points:
- Microphysical properties are retrieved with LIRIC from lidar and Sun photometer
- Uncertainties of LIRIC algorithm are evaluated for different conditions
- A unique set up with two Sun photometers at two altitude levels is used

Supporting Information:
- Supplementary Text
- Figure S1a
- Figure S1b
- Figure S1c
- Figure S2a
- Figure S2b
- Figure S2c
- Figure S2d
- Figure S3a
- Figure S3b
- Figure S3c
- Figure S3d
- Figure S4a
- Figure S4b
- Figure S4c
- Figure S4d
- Figure S5a
- Figure S5b
- Figure S5c
- Figure S5d

Correspondence to:
M. J. Granados-Muñoz,
mjgranados@ugr.es

Citation:
Granados-Muñoz, M. J., et al. (2014), Retrieving aerosol microphysical properties by Lidar-Radiometer Inversion Code (LIRIC) for different aerosol types, *J. Geophys. Res. Atmos.*, *119*, 4836–4858, doi:10.1002/2013JD021116.

Received 4 NOV 2013
Accepted 30 MAR 2014
Accepted article online 1 APR 2014
Published online 24 APR 2014

Retrieving aerosol microphysical properties by Lidar-Radiometer Inversion Code (LIRIC) for different aerosol types

M. J. Granados-Muñoz[1,2], J. L. Guerrero-Rascado[1,2], J. A. Bravo-Aranda[1,2], F. Navas-Guzmán[1,2,3], A. Valenzuela[1,2], H. Lyamani[1,2], A. Chaikovsky[4], U. Wandinger[5], A. Ansmann[5], O. Dubovik[6], J. O. Grudo[4], and L. Alados-Arboledas[1,2]

[1]Department of Applied Physics, Faculty of Sciences, University of Granada, Granada, Spain, [2]Andalusian Institute for Earth System Research (IISTA-CEAMA), Granada, Spain, [3]Now at Institute of Applied Physics (IAP), University of Bern, Bern, Switzerland, [4]Institute of Physics, National Academy of Science, Minsk, Belarus, [5]Leibniz Institute for Tropospheric Research, Leipzig, Germany, [6]Laboratory of Atmospheric Optics, University Lille 1, Villeneuve d'Ascq, France

Abstract LIRIC (Lidar-Radiometer Inversion Code) is applied to combined lidar and Sun photometer data from Granada station corresponding to different case studies. The main aim of this analysis is to evaluate the stability of LIRIC output volume concentration profiles for different aerosol types, loadings, and vertical distributions of the atmospheric aerosols. For this purpose, in a first part, three case studies corresponding to different atmospheric situations are analyzed to study the influence of the user-defined input parameters in LIRIC when varied in a reasonable range. Results evidence the capabilities of LIRIC to retrieve vertical profiles of microphysical properties during daytime by the combination of the lidar and the Sun photometer systems in an automatic and self-consistent way. However, spurious values may be obtained in the lidar incomplete overlap region depending on the structure of the aerosol layers. In a second part, the use of a second Sun photometer located in Cerro Poyos, in the same atmospheric column as Granada but at higher altitude, allowed us to obtain LIRIC retrievals from two different altitudes with independent Sun photometer measurements in order to check the self-consistency and robustness of the method. Retrievals at both levels are compared, providing a very good agreement (differences below 5 $\mu m^3/cm^3$) in those cases with the same aerosol type in the whole atmospheric column. However, some assumptions such as the height independency of parameters (sphericity, size distribution, or refractive index, among others) need to be carefully reviewed for those cases with the presence of aerosol layers corresponding to different types of atmospheric aerosols.

1. Introduction

Determination of the spatial-temporal variability of chemical, optical, and microphysical properties of atmospheric aerosols is still needed in order to reduce the uncertainties of their effects on the radiative forcing [*Forster et al.*, 2007; *Boucher et al.*, 2013]. Lidar systems have proved to be very useful tools for determining the vertical distribution of these aerosol properties. Vertical profiles of aerosol properties are of great importance since the atmospheric aerosol effects can be very different near the surface, within the boundary layer, and in the free troposphere.

Methods to determine aerosol optical properties with lidar systems have already been widely studied [*Klett*, 1985; *Ansmann et al.*, 1992]. However, the retrieval of aerosol microphysical properties represents still a real challenge, especially for nonspherical particles. These microphysical properties include their mean size, size distribution, volume, mass, surface area and number concentrations, and complex refractive index. Since the 1970s, several methods have been proposed in order to retrieve these microphysical properties, which can be classified basically in three different groups.

The first group consists of those methods based on the combination of a monostatic lidar with in situ instruments carried aboard, e.g., an aircraft [*Grams et al.*, 1972] or balloon [*Wandinger et al.*, 1995]. They present the major drawback that data from aircraft or balloons are not easily available, and they are obtained at very specific locations and time periods.

The second group consists of a mathematical approach on the basis of multiwavelength Raman lidar observations [*Uthe*, 1982; *Müller et al.*, 1999; *Veselovskii et al.*, 2002; *Böckmann et al.*, 2005]. This mathematical approach has proven to be quite robust for spherical particles [*Alados-Arboledas et al.,* 2011; *Navas-Guzmán et al.*, 2013a]. Nonetheless, recent publications extend this kind of methods to irregularly shaped particles, which are assumed to be a mixture of randomly oriented spheroids [*Veselovskii et al.*, 2010; *Müller et al.*, 2013]. These methods present the major advantage that no additional instrumentation is required, but they are mainly limited to nighttime operation since most of the current lidar systems do not offer Raman capabilities at daytime. In addition, these methods are based on undetermined set of equations and require a set of imposed constraints and the calculations of several set of solutions instead of a unique one. Also, these methods provide vertical profiles of the microphysical properties by layers, which imply a rather low vertical resolution in comparison with Lidar-Radiometer Inversion Code (LIRIC). In addition, the calculation of the vertical profiles by layers is quite time consuming, and an automatic robust implementation is not feasible.

The third group of methods is based on the synergic use of column-integrated aerosol properties information from passive remote sensing with vertical information derived from lidars. Some authors have developed methods in order to combine spaceborne column-integrated values with lidar vertical information [*Kaufman et al.*, 2003; *Léon et al.*, 2003], whereas in some other studies, the combined use of Sun photometer with lidar systems is proposed in order to derive vertically resolved aerosol microphysical properties [*Reagan et al.*, 1977; *Cuesta et al.*, 2008; *Chaikovsky et al.*, 2012; *Lopatin et al.*, 2013; *Wagner et al.*, 2013]. The combined use of information reduces the number of imposed constraints required in the mathematical approach used for the second group. However, there is a stringent requirement for such techniques that two collocated instruments provide measurements simultaneously. Since a few years such simultaneous data become available in an increasing number because there is an increasing tendency of equipping observation sites of such established networks as European Aerosol Research Lidar Network (EARLINET) [*Bösenberg et al.*, 2001] and Aerosol Robotic Network (AERONET) [*Holben et al.*, 1998] with both multiwavelength lidar systems and Sun photometers.

Within the frame of the European project ACTRIS (Aerosols, Clouds, and Trace Gases Research InfraStructure Network), one of the main objectives is to promote the development of the synergetic tools that combine AERONET Sun photometer measurements and EARLINET multiwavelength lidar data in order to obtain improved vertical profiles of aerosol microphysical properties. For this purpose, the retrieval algorithm LIRIC has been developed in the National Academy of Sciences of Belarus in collaboration with the Laboratoire d'Optique Atmosphérique, Lille (France) [*Chaikovsky et al.*, 2008, 2012]. LIRIC algorithm has already been presented and evaluated in previous studies [*Wagner et al.*, 2013], and the new and improved GARRLIC (Generalized Aerosol Retrieval From Radiometer and Lidar Combined) algorithm based on LIRIC fundamentals has already been developed [*Lopatin et al.*, 2013]. LIRIC has proven to be a relatively simple tool to retrieve aerosol microphysical properties profiles with high vertical resolution providing robust results [*Chaikovsky et al.*, 2012; *Wagner et al.*, 2013]. In the present work, the LIRIC algorithm is applied to lidar and Sun photometer data in order to obtain vertical profiles of aerosol volume concentration of both fine and coarse aerosol modes. The main contribution of this work is that for the first time, a quantitative analysis of the influence of the complete set of the different user-defined input parameters is studied with an emphasis on the possible effects of these parameters on LIRIC results under different atmospheric situations. In addition, a unique special observational setup has been used, namely, a second Sun photometer has been installed in the close vicinity of the main observational AERONET site but at higher altitude. This allowed us to obtain LIRIC retrievals from two different altitudes with independent Sun photometer measurements, providing a unique opportunity to check the LIRIC methodology and the quality of the LIRIC products under vertically varying aerosol conditions. Two study cases using such measurement configuration are presented here. In the first case, LIRIC is applied in a situation with a dust layer well mixed along the column and, in the second case, two different and clearly decoupled aerosol layers are investigated. Results allow comparing the profiles obtained from the two altitudes evaluating the performance of the algorithm under different atmospheric conditions.

2. Experimental Site and Instrumentation

This study was performed at the radiometric station of Granada (37.16°N, 3.61°W, and 680 meter above sea level (m asl)). Granada radiometric station is part of both EARLINET and AERONET networks. It is a

medium-size city in southeastern Spain with around 300,000 inhabitants, almost 500,000 including the metropolitan area. The city is located in a natural basin delimited by mountains, which can reach 3000 m asl at the east. Because of its location, 200 km away from Africa and around 50 km away from the western Mediterranean Basin, air masses are mainly coming from the Atlantic Ocean, Europe, North Africa, and the Mediterranean Basin [*Lyamani et al.*, 2005, 2006a, 2006b; *Alados-Arboledas et al.*, 2008]. The main aerosol sources in Granada are northern Africa, which is a major source of mineral dust [*Lyamani et al.*, 2005; *Valenzuela et al.*, 2012]; Europe as a source of anthropogenic pollution; and local sources, e. g., traffic and resuspension of material from the ground especially during the dry season [*Lyamani et al.*, 2006a, 2006b] and biomass burning [*Alados-Arboledas et al.,* 2011; *Navas-Guzmán et al.*, 2013b]. In winter, the domestic heating is a very important additional source of aerosols from anthropogenic origin.

The Raman lidar LR331D400 (Raymetrics S.A.) system is used in this study to measure vertical profiles of the atmospheric aerosol properties. This system is described in detail by *Guerrero-Rascado et al.* [2008, 2009]. It is a multiwavelength Raman system that emits at three different wavelengths (355, 532, and 1064 nm). The receiving system consists of several detectors, which can split the radiation according to the three elastic channels (355, 532, and 1064 nm), two nitrogen Raman channels (387 and 607 nm), and a water vapor Raman channel (408 nm). The system presents depolarization capabilities at 532 nm (532-cross and 532-parallel detection channels) [*Bravo-Aranda et al.*, 2013]. The Raman lidar was incorporated to EARLINET [*Bösenberg et al.*, 2001] in April 2005. It has been part of the EARLINET-ASOS (Advanced Sustainable Observation System) project (http://www.earlinet.org/) and currently is included in the ACTRIS European project (http://www.actris.net/).

A Sun photometer CIMEL CE-318-4 located in Granada radiometric station is used to obtain atmospheric aerosol properties integrated in the atmospheric vertical column [*Dubovik and King*, 2000; *Dubovik et al.*, 2006]. The automatic tracking Sun and sky scanning radiometer makes Sun direct measurements with a 1.2° full field of view every 15 min at 340, 380, 440, 500, 675, 870, 940, and 1020 nm (nominal wavelengths). These solar extinction measurements are used to compute aerosol optical depth (τ_λ) at each wavelength except for the 940 nm channel, which is used to retrieve total column water vapor (or precipitable water) [*Estellés et al.*, 2006; *Pérez-Ramírez et al.*, 2012]. The estimated uncertainty in computed τ_λ, due primarily to calibration uncertainty, is around 0.01–0.02 for field instruments (which is spectrally dependent, with larger errors in the UV) [*Eck et al.*, 1999; *Estellés et al.*, 2006]. The Sun photometer located in Granada is included in the AERONET-RIMA network (Iberian Network for Aerosol Measurements, federated to AERONET) (http://www.rima.uva.es/index.php/en/) since 2002, and it is calibrated every year [*Valenzuela et al.*, 2012].

A second Sun photometer CIMEL CE-318-4 is located in Sierra Nevada, 12 km away (horizontally) from Granada, at the Cerro Poyos station (37.11°N, 3.49°W, and 1820 m asl). This Sun photometer is also included in AERONET since 2011 through RIMA, operating mainly during summertime, and it is also calibrated once a year. Considering the short horizontal distance to the Granada station (12 km), it is assumed that both Sun photometers observe the same atmospheric column [*Alados-Arboledas et al.*, 2008].

3. Methodology

3.1. Brief Description of LIRIC Algorithm

The Lidar Radiometer Inversion Code is used in this study. In this section, a brief and schematic description of the code (version October 2012) is provided. More details and an exhaustive description of the equations can be found in previous studies [*Chaikovsky et al.*, 2008, 2012; *Kokkalis et al.*, 2013; *Wagner et al.*, 2013].

LIRIC is a retrieval algorithm that provides profiles of atmospheric aerosol microphysical properties from the combination of elastic lidar signals and radiometer measurements. Figure 1 schematically shows LIRIC's structure.

The main LIRIC inputs are atmospheric aerosol columnar optical and microphysical properties retrieved from direct Sun and sky radiance measurements from the radiometer using the AERONET code (version 2, level 1.5) [*Dubovik et al.*, 2006] and measured lidar elastic backscatter signals. These elastic lidar signals are included as raw files with specifications that are used by LIRIC for preprocessing corrections (background, dark current, and dead time). Based on original LIRIC setup, lidar elastic signals at three different wavelengths (355, 532, and 1064 nm) are required for providing robust retrieval of vertical aerosol profiles. If available, also the

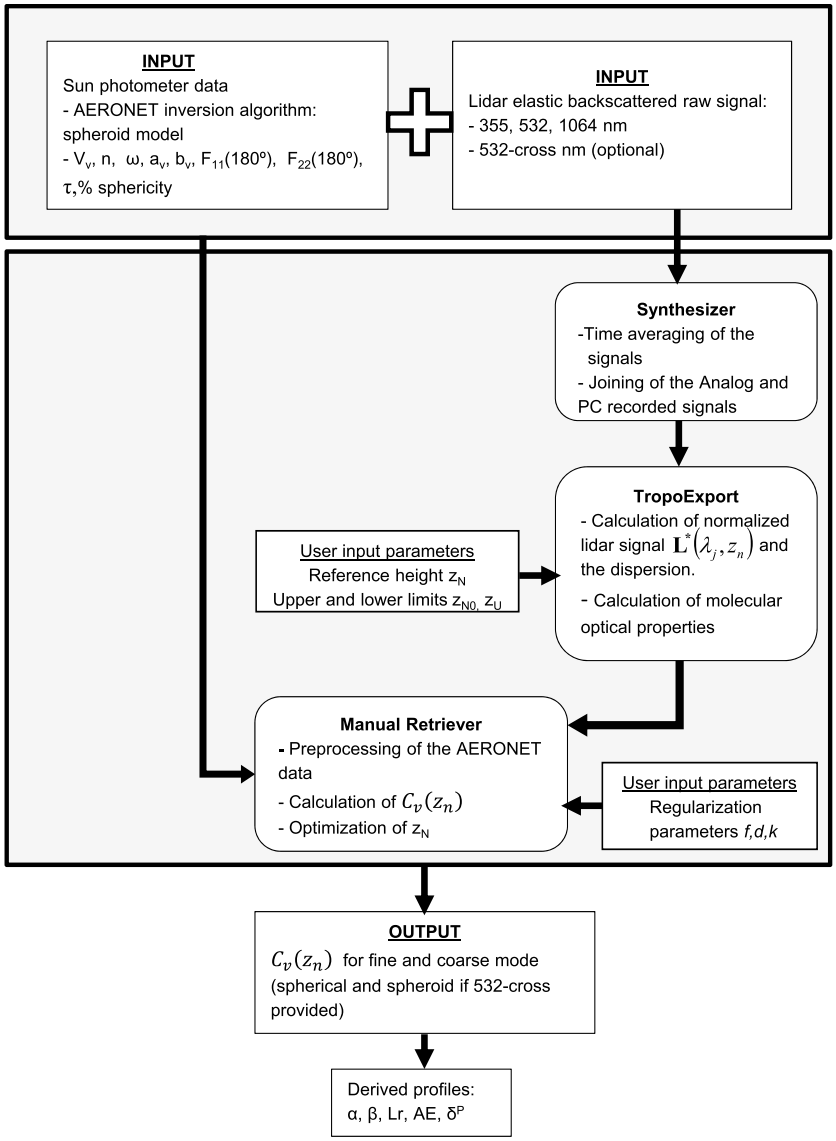

Figure 1. Schematic description of LIRIC algorithm. Lidar elastic signals at different wavelengths (355, 532, and 1064 nm and if available 532 nm cross-polarized) and AERONET inversion products are used as input data in the software. Lidar signals are preprocessed in Synthesizer and TropoExport to obtain $L^*_\lambda(z_n)$, which is used as input in manual retriever together with the AERONET version 2, level 1.5 data recalculated for the lidar wavelengths. Main outputs are the volume concentration profiles $C_v(z_n)$ for the fine and coarse mode. If 532 nm cross-polarized lidar signal is available as input, the output $C_v(z_n)$ is retrieved for the fine, coarse spherical, and coarse spheroid modes. From $C_v(z_n)$ profiles and column-integrated properties, optical properties profiles such as the aerosol backscatter coefficient $\boldsymbol{\beta}$, the aerosol extinction coefficient α, the lidar ratio, the Angström exponent, or the particle linear depolarization ratio δ^P can also be calculated. See text for more information on input parameters.

532 nm cross-polarized signal is used. From the combination of all these data, volume concentration profiles $C_v(z_n)$ are obtained distinguishing between fine and coarse aerosol particles. For this purpose, based on the AERONET code, an aerosol model, defined by the columnar integrated volume concentrations V_v of each mode (fine and coarse modes) and based on a mixture of randomly oriented spherical and spheroid particles, is assumed as described by *Dubovik and King* [2000] and *Dubovik et al.* [2006]. The separation between the fine and the coarse modes is made using the AERONET-retrieved bimodal aerosol volume size distribution. The separation radius is located at the minimum of the distribution in the radii range between 0.194 and 0.576 μm. The use of the 532 nm cross-polarized lidar channel allows for distinguishing spherical and

nonspherical particles within the coarse fraction of the aerosol. As the lidar system LR331D400 has depolarization capabilities and the 532 nm cross-polarized lidar data are available, in this study volume concentration profiles $C_v(z_n)$ will be retrieved for fine, coarse spherical, and coarse spheroid modes. Anyway, the sum of the volume concentrations for the coarse spherical and coarse spheroid modes is compared with the total coarse mode obtained when the 532 nm cross-polarized channel is not taken into account, in order to evaluate the performance of the algorithm when using different input data.

LIRIC software is composed of a number of modules for the processing of the lidar and Sun photometer data described by *Chaikovsky et al.* [2012]. One of these modules included in LIRIC is the so-called TropoExport. In this part, the molecular optical properties are calculated assuming either a standard atmosphere or a user-defined one. Lidar data are normalized here in order to obtain the profile denoted as $L^*_\lambda(z_n)$. $L^*_\lambda(z_n)$ is obtained by normalizing the experimental lidar range corrected signal as explained by *Chaikovsky et al.* [2008] and will be used as input for the retrieval of microphysical properties. For the normalization of the lidar signals, it is necessary to assume a calibration height, z_N, corresponding to an aerosol-free region. The value of z_N is selected by the user in TropoExport. In this module, also, the upper and lower height limits of the lidar signals, where it is considered to be reliable, are indicated. The lower height limit, z_{N0}, is chosen at that height above, which lidar data are considered not to be influenced by the incomplete overlap. Below this lower limit, the volume concentration is assumed to be constant down to the surface. Therefore, $C_v(z_n) = C_v(z_{N0})$ if $z_n < z_{N0}$. The upper limit, z_U, is established at a height where no aerosol is found and only molecular signal is expected, always above the reference height. TropoExport module also calculates the statistical dispersion of $L^*_n(z_n)$ as explained by *Chaikovsky et al.* [2008].

The retrieval of the microphysical properties itself is performed in the Manual Retriever module of LIRIC, using as input $L^*_\lambda(z_n)$ and the Sun photometer optical and microphysical properties recalculated for the working wavelengths of the lidar system, according to *Dubovik et al.* [2006]. The retrieval is based on a set of three equations for every wavelength described in detail by *Chaikovsky et al.* [2008].

In this module of the software, the so-called regularization parameters (*k, f,* and *d*) can be adjusted by the users and strongly affect the output profiles. They supply new information in order to avoid spurious solutions and optimize the output profiles. Specifically, the regularization parameter *k* is related to lidar measurement as well as aerosol layer properties, the parameter *f* is related to radiometric measurements, and the parameter *d* regulates the smoothness of the concentration profile. In order to obtain the output profiles, an iterative procedure based on the Levenberg–Marquardt method is applied in LIRIC, as shown by *Chaikovsky et al.* [2008]. Once the $C_v(z_n)$ profiles are obtained, the backscatter ratio at the reference height z_N is optimized.

The main outputs of LIRIC are the volume concentration profiles $C_v(z_n)$ for the different modes (fine, coarse spherical, and coarse spheroid in this study). However, from these profiles, it is also possible to obtain some other derived properties such as the aerosol backscatter and extinction coefficient profiles or the particle linear depolarization ratio (δ^P), that informs about the aerosol particle shape. Aerosol backscatter and extinction coefficient profiles and particle linear depolarization ratio profiles are calculated as in *Wagner et al.* [2013].

3.2. Uncertainties of the Algorithm

This section discusses the methodology used to analyze the uncertainties in LIRIC output volume concentration profiles $C_v(z_n)$ due to the variations in the user-defined input parameters. It is necessary to point out that the uncertainties of the input elastic lidar signals and AERONET data were not taken into account in this analysis. These uncertainties are around 15%, considering the statistical uncertainties retrieved with Monte Carlo techniques for the case of the lidar data according to *Pappalardo et al.* [2004] and *Guerrero-Rascado et al.* [2008]. In the case of AERONET data, these uncertainties are quite variable for the different optical and microphysical properties retrieved, i.e., τ_λ uncertainty ranges from ±0.01 in the infrared visible to ±0.02 in the ultraviolet channels [*Eck et al.*, 1999], and the uncertainty in the retrieval of $\omega(\lambda)$ is ±0.03 with high-aerosol load ($\tau_{440\,\mathrm{nm}} > 0.4$) and 0.02–0.07 with low-aerosol load ($\tau_{440\,\mathrm{nm}} < 0.2$). The reported uncertainties are around 10–35% for the aerosol size distribution retrievals in the $0.1\ \mu\mathrm{m} < r < 7\ \mu\mathrm{m}$ size range, while for size retrieval outside of this range, uncertainties rise up to 80–100%. More details can be found in *Dubovik and King* [2000] and *Dubovik et al.* [2002, 2006]. Therefore, only uncertainties in the output profiles due to LIRIC algorithm itself

are quantified. For this purpose, different sets of user-defined parameters have been tested for different atmospheric aerosol types and loads in order to evaluate the stability of the retrieved volume concentration profiles. Specifically, the user-defined parameters that will be evaluated are the reference height z_N, the lower limit height z_{N0}, the upper limit z_U, and the regularization parameters k, f, and d. Values of these parameters are varied within their uncertainty limits in a reasonable range.

3.2.1. Lower Limit Height z_{N0}

As previously stated, the lower limit height is chosen at that altitude where the lidar signal is considered not to be affected by incomplete overlap. To study the influence of the variations in z_{N0} on the $C_v(z_n)$ profiles, three different retrievals with three different values of z_{N0} were performed for each case. These values are chosen in the altitude range between 400 and 1000 m above the lidar system, where the overlap is larger than 80% [*Navas-Guzmán et al.*, 2011].

3.2.2. Reference Height z_N

The reference height has to be chosen in an aerosol-free region, where only molecular signal is expected. As in previous studies [*Wagner et al.*, 2013], the reference height was chosen at a level where the backscatter ratio (total to molecular backscatter ratio) is lower than 1.1 for each wavelength to guarantee that the aerosol backscattered signal is less than 10% of the molecular one. Three different retrievals with different values corresponding to three reference heights separated 200 m were performed for each case in order to evaluate the influence of this parameter in the final output. The difference between the z_N values was chosen to be 200 m, because no significant fluctuations were expected in the volume concentration profiles for lower values. Nonetheless, tests with higher distances (up to 400 m) were performed in some cases. It was observed that the uncertainties were very similar to those obtained with 200 m, except for some specific situations that will be explained later.

The reference height z_N is a priori defined by the user; however, LIRIC optimizes the backscatter ratio at this altitude and performs an internal procedure to consider the possible contribution of aerosol backscattering from the reference layer. Therefore, low variations are expected in the final output if the algorithm adequately corrects the backscatter ratio at z_N.

3.2.3. Upper Limit Height z_U

The upper limit is established at a height where no aerosol is found. Due to software constraints, the upper limit has to be always above the reference height z_N. Above the upper limit, no profiles are retrieved anymore. In order to study the influence of the upper limit in the retrieval of $C_v(z_n)$, three different heights are used as input data for three different retrievals. As no aerosol is expected to be at heights above z_U, the output $C_v(z_n)$ are not expected to substantially change with this parameter.

3.2.4. Regularization Parameters

Different sets of values for the regularization parameters k, f, and d are used in order to perform several retrievals and evaluate the uncertainties they introduce in the final $C_v(z_n)$ profiles. The regularization parameters k and f are varied by several orders of magnitude, but always satisfying that the column-integrated volume concentration values of each mode do not differ by more than 5% from those provided by AERONET. Parameter d is varied from 1 to 5.

The results of the stability tests applied to the three different cases, corresponding to different aerosol types, loads, and vertical distributions, are shown in section 4.

3.3. Comparison of the Optical Properties Profiles

Aerosol backscatter coefficient profiles calculated from $C_v(z_n)$ are compared with those calculated with the Klett–Fernald algorithm from the lidar data [*Fernald et al.*, 1972; *Klett*, 1981, 1985; *Fernald*, 1984]. This algorithm retrieves the aerosol backscatter coefficient profiles corresponding to the elastic wavelengths assuming a reference height free of aerosol particles and a height independent aerosol lidar ratio for each wavelength. More details can be found in *Bravo-Aranda et al.* [2013] and *Guerrero-Rascado et al.* [2009, 2011]. Lidar ratios assumed when applying the Klett–Fernald algorithm to the lidar data are obtained by minimizing the difference between the integral of the aerosol backscatter coefficient profile multiplied by the lidar ratio and the aerosol optical depth provided by AERONET for each wavelength [*Guerrero-Rascado et al.*, 2008]. It is necessary to take into account that the assumption of a constant lidar ratio introduces some uncertainty in the lidar-retrieved aerosol backscatter coefficient profiles [*Sasano et al.*, 1985]. On other hand, δ^P profiles at 532 nm retrieved using the 532-parallel and 532-cross profiles measured with the lidar system will be

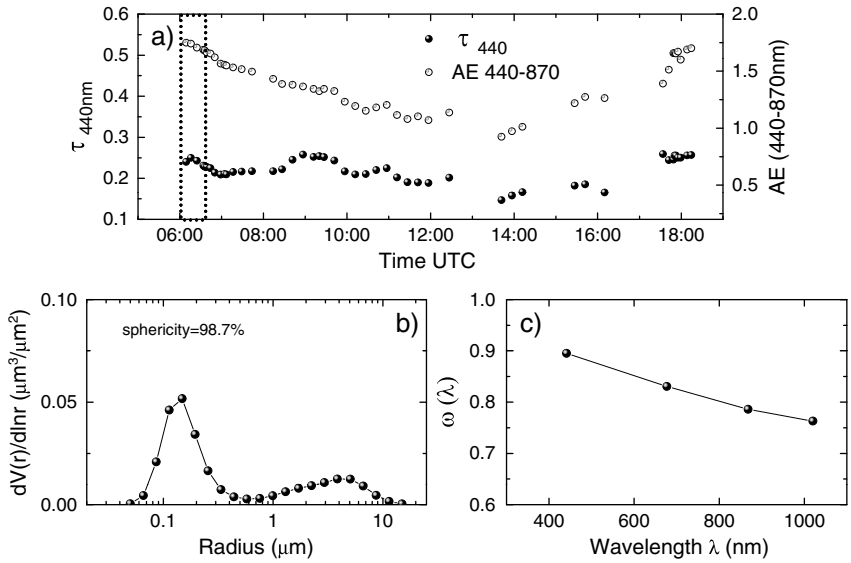

Figure 2. (a) Time series of AERONET τ_{440} and AE(440–870 nm) data on 22 May 2011. The dotted rectangle indicates the period analyzed with LIRIC. (b) Volume size distribution retrieved by AERONET inversion algorithm version 2, the same day at 06:25 UTC. (c) Single scattering albedo $\omega(\lambda)$ versus wavelength λ retrieved by AERONET for the same date.

compared with those retrieved from the $C_v(z_n)$ profiles obtained with LIRIC. In order to retrieve the accurate δ^P profiles from lidar measurements, a careful calibration of the instrument is required [*Bravo-Aranda et al.*, 2013]. Thus, it is necessary to take into account the polarizing effects associated to the different optical elements (e.g., effective diattenuation of the optical systems) and the misalignment between the polarization plane of the laser and the optical devices. In this way, we use procedures described by *Freudenthaler et al.* [2009] and *Bravo-Aranda et al.* [2013]. These profiles are compared with those retrieved from the $C_v(z_n)$ profiles obtained with LIRIC according to equations in *Wagner et al.* [2013]. In order to understand our results, it is also necessary to take into account that δ^P profiles retrieved from LIRIC depend on the fraction of spherical particles provided by AERONET, which presents a significant uncertainty especially in cases of very weak or very strong depolarizing aerosol layers, thus reducing the reliability of δ^P profiles based on LIRIC retrievals.

4. Evaluation of LIRIC Performance

4.1. Case Study I: Pollution Episode on 22 May 2011

On 22 May 2011, a pollution episode was observed at Granada. A backward trajectory analysis performed with Hybrid Single Particle Lagrangian Integrated Trajectory (HYSPLIT) model [*Draxler and Rolph*, 2003] indicated southern Europe as the origin of the air masses arriving at Granada below 4 km asl (Figure S1b in the supporting information). This European region and specially the Po Valley, in Northern Italy, are highly polluted areas and important source regions of anthropogenic pollution [*Barnaba and Gobbi*, 2004]. The NAAPS (Navy Aerosol Analysis and Prediction System) model [*Christensen*, 1997] forecast the presence of sulphates over the Iberian Peninsula (Figure S1c in the supporting information), which is also an indicator of anthropogenic pollution.

AERONET data obtained during this episode are presented in Figure 2. The Angström exponent between 440 and 870 nm, AE(440–870 nm), obtained from the Sun photometer data indicated values along the day ranging from 0.9 to 1.8, which are related to the predominance of small particles (Figure 2a). This predominance was confirmed by the size distribution retrieved at 06:25 UTC, which shows much larger-concentration values for the fine mode (Figure 2b). The AE(440–870 nm) at this time was 1.8, and the fine mode fraction was 0.85. The $\omega(\lambda)$ values retrieved at the same time showed a decreasing tendency with λ, which is typical of polluted conditions [*Dubovik et al.*, 2002; *Lyamani et al.*, 2006b] (Figure 2c). The aerosol load however was not very high, as deduced from τ_{440} values (~0.20) (Figure 2a).

Table 1. Starting Sets of User-Defined Input Parameters for LIRIC Retrievals for the Study Cases I, II, and III (z_{N0} = Lower Limit, z_N = Reference Height, z_U = Upper Limit, k_λ = Lidar Regularization Parameters, f_v = Sun Photometer Regularization Parameters, and d_v = Smooth Constraints Regularization Parameters[a]

	Case I: Pollution Episode	Case II: Mineral Dust Event	Case III: Mixture of Aerosol Types
Date	22 May 2011	3 Aug 2012	10 Sept 2012
z_{N0} (m asl)	1010	1080	1175
z_N (m asl)	4000	6000	3750
z_U (m asl)	4150	6150	3900
k_{335}	$2.5 \cdot 10^{-4}$	$1.5 \cdot 10^{-5}$	$7.5 \cdot 10^{-5}$
k_{532}	$7.5 \cdot 10^{-4}$	$5 \cdot 10^{-6}$	$5 \cdot 10^{-5}$
k_{1064}	$2.5 \cdot 10^{-4}$	$2.5 \cdot 10^{-6}$	$2.5 \cdot 10^{-5}$
k_{532c}	$7.5 \cdot 10^{-5}$	$7.5 \cdot 10^{-7}$	$7.5 \cdot 10^{-5}$
f_{fine}	5	0.2	1
$f_{\text{spherical}}$	25	0.2	1.5
f_{spheroid}	5	0.2	0.5
d_{fine}	5	1	5
$d_{\text{spherical}}$	5	1	1
d_{spheroid}	5	1	1

[a]Heights are expressed in m asl, and regularization parameters are unitless.

Results from AERONET presented in Figure 2 are combined with lidar elastic signals at 355, 532, and 1064 nm and the 532 nm cross-polarized signal in order to retrieve the microphysical properties profiles with LIRIC algorithm. Lidar data are averaged between 06:00 and 06:30 UTC. A first retrieval was performed using the starting set of user-defined input parameters listed in Table 1.

From this starting set of user-defined input parameters, variations described in section 3.2 were applied here in order to study the influence of the different parameters in the final obtained profiles. As the volume concentration of the coarse spheroid mode was zero, only the results of fine and coarse spherical modes are presented here.

First, the influence of variations in the user-defined lower limit, z_{N0}, was analyzed. Three different retrievals with LIRIC were performed using three different values of z_{N0} (1010, 1200, and 1400 m asl) and keeping all the other parameters as in Table 1. The profiles in Figure 3a represent the mean values of the profiles

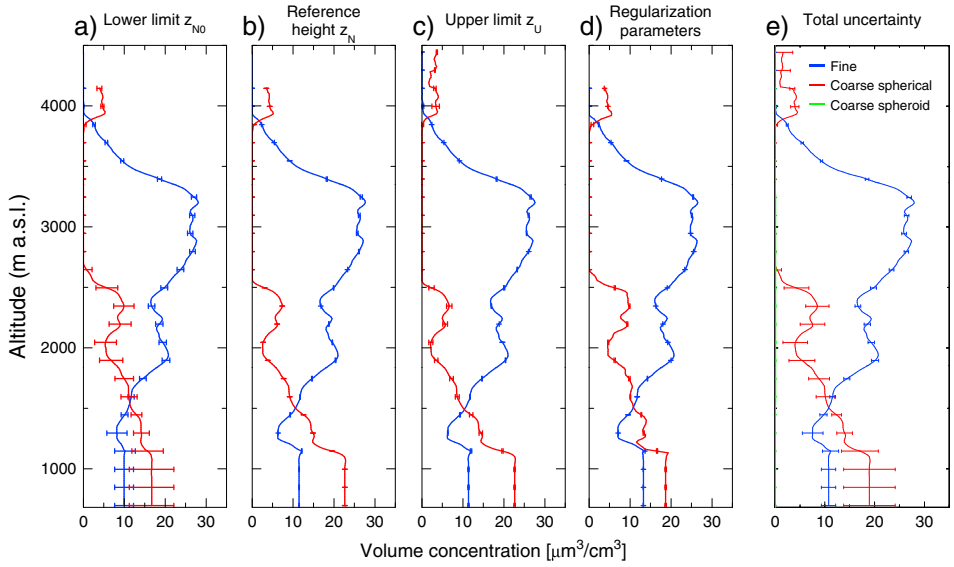

Figure 3. Mean fine (blue), coarse spherical mode (red), and coarse spheroid (green) volume concentration profiles and standard deviations (error bars) on 22 May 2011 between 06:00 and 06:30 UTC obtained by performing different retrievals varying (a) z_{N0}, (b) z_N, (c) z_U, and (d) regularization parameters, as indicated in the text. (e) Mean profiles and standard deviation obtained by averaging all the previous profiles.

obtained from the three different retrievals, and the bars indicate one standard deviation, which is considered as the uncertainty. Variations of the lower limit height value produced larger uncertainties in the lower part of the profile, with values up to 25% for the fine mode and 33% for the coarse spherical mode. In the upper part of the profile, above 1500 m asl uncertainties were around 20% for the coarse spherical mode and below 10% for the fine mode.

Uncertainties due to variations in the reference height z_N were also analyzed (Figure 3b). Three different retrievals were performed keeping the upper and lower limits and the regularization parameters unchanged and using three different values for z_N (4000, 4200, and 4400 m asl). The uncertainties produced by the changes in the reference height are of the order of 1% in both profiles, fine and coarse spherical. The low uncertainty indicates that LIRIC internally considers the possible contribution of aerosol backscattering for the reference height and correctly converges to an optimal solution, proving that the algorithm is robust under these conditions.

Figure 3c shows the profiles and the uncertainties obtained by varying the upper limit height z_U values. Three different values were used between 4150 and 4550 m asl in the three different retrievals performed. The obtained uncertainties were around 1% in the whole profile except for the upper part, above 4 km asl, where uncertainties reached 25% in the coarse spherical mode. This larger uncertainty is due to the presence of an unrealistic positive offset observed in the molecular height range above the aerosol layers. LIRIC tends to introduce a positive offset in the volume concentration profiles $C_v(z_n)$ indicating the presence of aerosol particles at these levels, where there is no aerosol backscattering according to the lidar data, and affecting the whole retrieved profiles $C_v(z_n)$. This offset was also observed in previous studies [*Wagner et al.*, 2013]. In order to avoid additional uncertainties due to the presence of this offset, the upper limit should be kept as low as possible, and consequently, the same must be done with the reference height z_N. For the regularization parameters, values were changed by increasing or decreasing 1 order of magnitude, the original *k* and *f* parameters. Several combinations were used either simultaneously increasing (or decreasing) *k* and *f* or either simultaneously increasing *k* and decreasing *f* values (or vice versa). The regularization parameter *d* was varied between 1 and 5. A total of five different sets of regularization parameters were used to perform five retrievals, but always satisfying that the column-integrated volume concentration of each mode did not differ more than 5% of the ones provided by AERONET, as indicated before. For this case, the variation in the regularization parameters introduced almost no uncertainties (just around 1% for the whole profile).

Summarizing, the largest uncertainties were obtained for the variations in the lower limit height z_{N0}, especially in the lower part of the profile (below 1500 m asl). Variations were larger for the coarse spherical mode. Uncertainties due to variations for the other three input parameters tested were very similar with values around 1% for both modes.

Figure 3e shows the mean profiles and the standard deviations obtained from the 14 previous retrievals, calculated by averaging the results of all the profiles obtained in each step of the stability test. These mean profiles and standard deviations account for the total uncertainty introduced by all the user-defined input parameters. Relative errors were very low (below 5%) in the case of the fine mode concentration values. However, in the lower part of the profile, larger relative deviations were found (up to 30%). The coarse spherical mode volume concentration profile had relative errors around 20%, except for the region affected by overlap. In the case of volume concentration values below 10 $\mu m^3/cm^3$, the relative error reached 30%.

The obtained $C_v(z_n)$ profiles indicated the existence of both fine and coarse spherical particles up to 2500 m asl, whereas an absolute predominance of the fine mode is obtained from 2500 m up to 4000 m asl. No concentration should be observed above the reference height z_N. However, the retrieval indicates that there are some coarse spherical particles above z_N. This is due to the unrealistic offset introduced by the algorithm in the molecular height range, as reported by *Wagner et al.* [2013]. The fine mode however is not affected by offsets in this case.

The coarse spherical mode volume concentration profile retrieved for this case is equivalent to the one obtained for the total coarse mode when performing the retrieval without using the 532 nm cross-polarized channel, with differences below 5%. The fine mode profile differences are even lower for both retrievals (with and without 532 nm cross-polarized information).

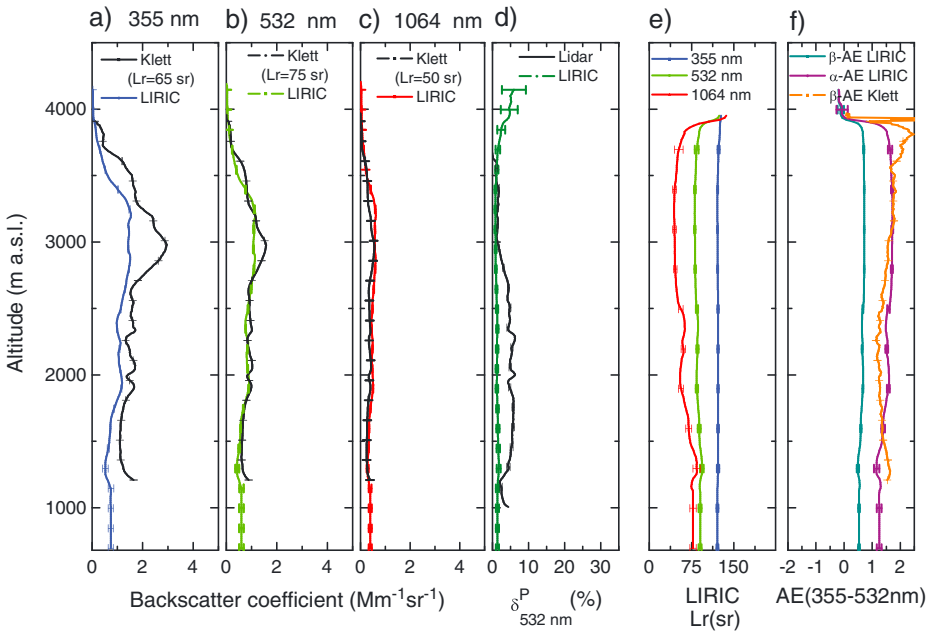

Figure 4. Aerosol backscatter coefficient profiles at (a) 355 nm, (b) 532 nm, and (c) 1064 nm retrieved from LIRIC output profiles (colored lines) and Klett–Fernald–Sasano (black lines) on 22 May 2011 between 06:00 and 06:30 UTC. (d) δ^P profiles obtained from LIRIC (coloured line) and lidar data (black line) for the same period. (e) Lidar ratio profiles obtained from LIRIC retrievals. (f) Backscatter and extinction related Angström exponent between 355 and 532 nm profiles retrieved with LIRIC and backscatter-related Angström exponent obtained with Klett–Fernald–Sasano. The error bars of LIRIC profiles indicate the standard deviations obtained from the 14 retrievals performed as indicated in section 3.2.

Figure 4 shows the comparison between aerosol optical properties retrieved by applying Klett–Fernald inversion algorithm to lidar data and those calculated from the volume concentration profiles retrieved by means of LIRIC. As explained in section 3.2, the lidar ratio assumed in the Klett–Fernald retrieval is obtained from the comparison between the integrated aerosol extinction coefficient from lidar profiles and the Sun photometer aerosol optical depth. The agreement in the aerosol backscatter coefficient profiles was better for 532 and 1064 nm. For 355 nm, differences were much larger, especially around the maximum at 3000 m asl. Important discrepancies were also found between the lidar ratio at 355 nm (65 sr) considered for the Klett–Fernald retrieval and the lidar ratio profile obtained from LIRIC with a mean value of around 120 sr. This lidar ratio value is very large compared to the usual values provided in the literature [e.g., *Amiridis et al.*, 2005; *Müller et al.*, 2007; *Preißler et al.*, 2013]. Only in those cases of highly polluted episodes lidar ratios reach values above 100 sr [e.g., *Franke et al.*, 2001; *Mattis et al.*, 2004]. However, for the 532 nm, channel values were quite similar for both methods (~75 sr). Differences between lidar ratios were also considerable for 1064 nm. However, as the dependence of the retrieved aerosol backscatter coefficient on the assumed lidar ratio in the Klett–Fernald method decreases with wavelength [*Wiegner and Geiß*, 2012], this difference is not significant.

The extinction-related Angström exponent profile, α-AE, provided by LIRIC and the backscatter-related Angström exponent profile, β-AE, obtained with Klett–Fernald (Figure 4f) presented a very good agreement with the AERONET column-integrated Angström exponent values (~1.5). However, β-AE profile retrieved with LIRIC presented very low values ($<$0.75) in comparison with that derived using the Klett–Fernald algorithm. Therefore, according to the retrieved Angström exponent profiles, the discrepancies observed in the lidar ratios markedly affect the aerosol backscatter coefficient profiles retrieved with LIRIC. This is in agreement with the fact that α-AE is related to β-AE through the equation α-AE = β-AE + Lr-AE, where Lr-AE is the lidar ratio related Angström exponent [*Ansmann et al.*, 2002]. The unusual values obtained in the Lr-AE retrieved by AERONET compared with the literature lead to inconsistent values retrieved with LIRIC for the β-AE.

The δ^P profile obtained by using the lidar profiles and the appropriate calibration following *Bravo-Aranda et al.* [2013] was around 7% below 2.5 km and close to 0% above this altitude, indicating a predominance of spherical particles in the whole layer. LIRIC-derived δ^P was very constant, with values around 0% indicating

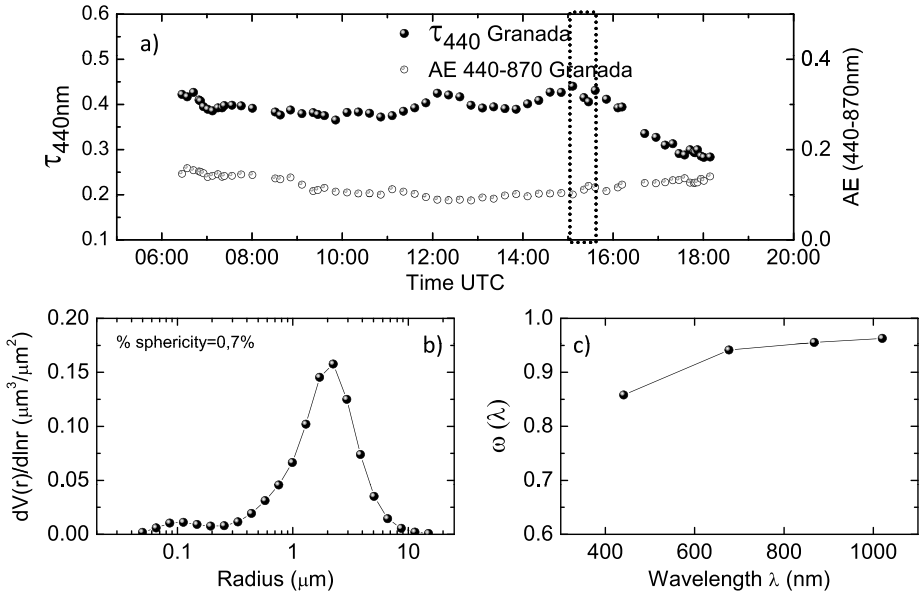

Figure 5. As in Figure 4 but for the 3 August 2012. AERONET inversion data correspond to 15:22 UTC.

no contribution of spheroid particles, as it can be seen in the volume concentration profiles. Above 3 km asl, the agreement between both δ^P profiles obtained was quite good. However, below 3 km asl, discrepancies are higher, with δ^P provided by the lidar around 7% and the one obtained with LIRIC almost negligible. Thus, LIRIC δ^P profiles presented both lower and more constant values than those retrieved using the approach proposed by *Bravo-Aranda et al.* [2013]. These features, especially the underestimation of the LIRIC δ^P profiles, are also evident in the analyses of *Wagner et al.* [2013]. These differences are originated in the different procedures followed in each one of the retrievals. LIRIC combines AERONET information on the sphericity for the whole column and cross and parallel raw profiles at 532 nm. Meanwhile, our procedure uses these last profiles including a careful calibration, which corrects misalignment between the polarization plane of the laser and the optical system and diattenuation effects of the lidar system. This last information is not included among the system input parameters provided to LIRIC for preprocessing, although LIRIC takes into account the possibility of cross talking between the parallel and perpendicular signals. In addition, LIRIC δ^P profiles are affected by a high uncertainty in this case of a very low depolarizing aerosol in the atmospheric column.

4.2. Case Study II: Mineral Dust Event on 3 August 2012

A mineral dust event occurred at the city of Granada on 3 August 2012. Backward trajectory analysis revealed the origin of the air masses in North Africa above 3 km. However, for lower altitudes, the air masses had its origin over the Atlantic Ocean and the Iberian Peninsula (Figure S2b in the supporting information). NAAPS model forecast the presence of mineral dust over the southeastern Iberian Peninsula and also sulphates and smoke in close areas (Figure S2c in the supporting information). BSC-DREAM8b forecast model indicated the presence of mineral dust over the Iberian Peninsula, but the dust loading values were relatively low (Figure S2d in the supporting information).

According to the Sun photometer data (Figure 5), there were high-aerosol loadings along the whole day, with τ_{440} values over 0.40 during the morning and slightly decreasing to 0.2 during the afternoon. The AE(440–870 nm) was around 0.1 during the whole day, and the fine fraction was 0.16, indicating the predominance of coarse particles. The $\omega(\lambda)$ values retrieved from AERONET inversions at 15:22 UTC presented values over 0.85 increasing with λ, which is the characteristic spectral dependence of $\omega(\lambda)$ under dust conditions [*Dubovik et al.*, 2002; *Alados-Arboledas et al.*, 2008; *Valenzuela et al.*, 2012]. The size distribution for the same time period showed a clear predominance of the coarse mode with high-concentration values.

Lidar data between 14:30 and 15:00 together with AERONET inversion at 15:22 UTC are the input data used for LIRIC retrieval. A first retrieval was performed using the input parameters described in Table 1 for

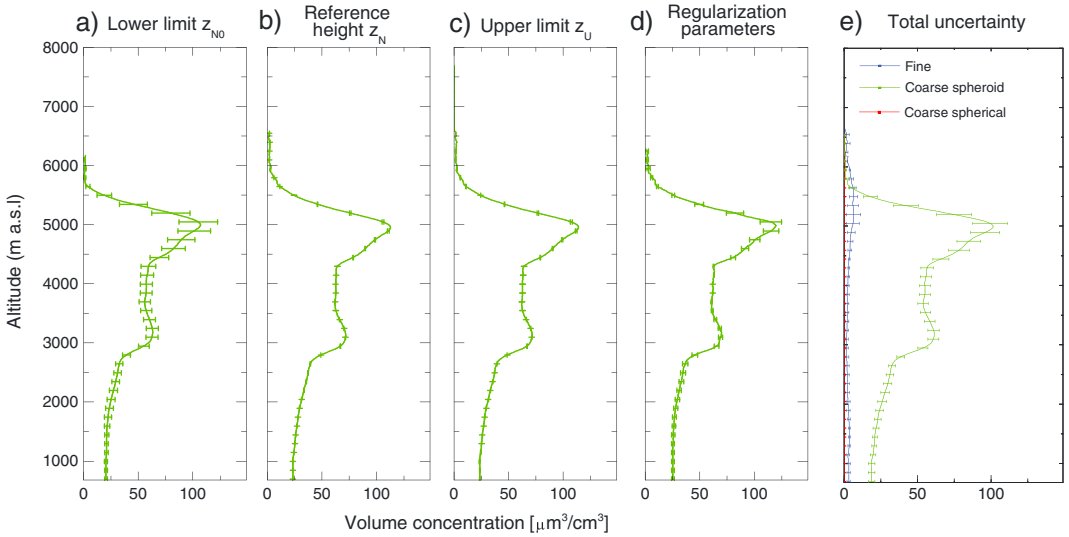

Figure 6. As in Figure 3 but for 3 August 2012.

3 August 2012 and then retrievals with variations of the user-defined input parameters as described in section 3.3 were also obtained. As no coarse spherical and almost no fine particles were obtained, only results of the test applied to the coarse spheroid mode volume concentration profile are shown here. Figure 6a shows the mean profile and the standard deviations (represented by the error bars) of the coarse spheroid volume concentration profile obtained from three different retrievals varying z_{N0} values (1080, 1280, and 1520 m asl). As in the previous case, the variations of z_{N0} produced quite high uncertainties in the profile, up to 25%. However, in this case, maximum uncertainties were observed at 5000 m asl, where the maximum concentration was obtained and not in the lower part of the profile.

Figure 6b shows the uncertainties calculated varying the reference height (6000, 6200, and 6400 m asl) and keeping unchanged the other input parameters as in Table 1. The uncertainties reached maximum values of ~2%, indicating that LIRIC properly corrects the possible influence of aerosol backscatter at the reference height. It is interesting to point out that in this case, when varying z_N up to 6800 m asl, uncertainties around 17% appeared in the profile. This did not occur in the other two cases presented here. This could be an indicator that the internal correction of the backscatter ratio at the height z_N presents some difficulties at high altitudes due to the low signal-to-noise ratio.

For z_U, 6150, 6350, and 6550 m asl values were used. The obtained uncertainties were very similar to those obtained by varying the reference height. The unrealistic offset observed in the previous case is much lower in this case for the spheroid mode.

For the regularization parameters (Figure 6d), values were changed just as in the previous case. The different values of the regularization parameters used lead to rather low standard deviations, with values around 10%.

For the lower limit and the regularization parameters, the largest uncertainties appeared always in the maximum located around 5 km asl. The lowest uncertainties were obtained when varying z_N and z_U,and the highest uncertainties were again obtained for the variations in the lower limit height z_{N0} values.

Figure 6e shows the averaged profiles obtained from the 14 retrievals obtained in the varying input parameters and represented in Figures 6a–6d. Relative errors are below 20% in the whole profile, with maximum values around 5 km asl.

The volume concentration profiles clearly indicate a predominance of the coarse spheroid mode, with larger concentration values between 2.7 and 5.6 km asl. A maximum of 90 $\mu m^3/cm^3$ was obtained around 5 km asl. Also, some fine particles were found along the profile, but its volume concentration was almost negligible (10 $\mu m^3/cm^3$ at a maximum around 5.1 km asl) compared to the coarse spheroid mode. As in the

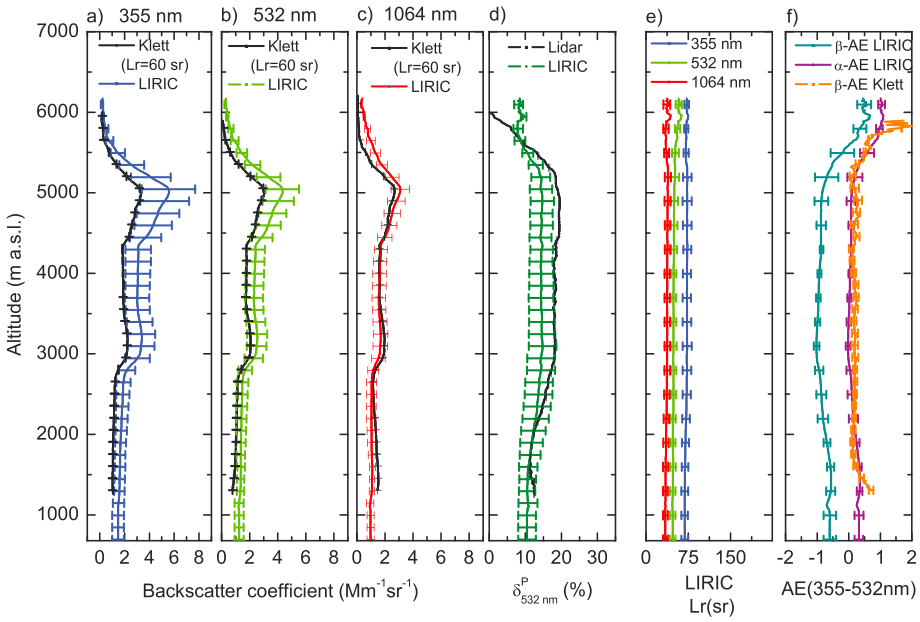

Figure 7. As in Figure 4 but for 3 August 2012.

previous case, the total coarse mode, retrieved without including the 532 nm cross-polarized channel, is in agreement with the coarse spheroid mode shown in Figure 6e, with discrepancies below 2%.

Figure 7 shows the aerosol backscatter coefficient profiles obtained by Klett–Fernald from the lidar data and those retrieved from the volume concentration profiles retrieved by LIRIC. Agreement in this case was much better for 532 and 1064 nm than for 355 nm. An unusual increase of the aerosol backscatter coefficient with wavelength was observed for the profiles retrieved with LIRIC, with the largest values for 1064 nm and the lowest for 355 nm, which in turn led to negative β-AE profiles (Figure 7f). However, this unusual wavelength dependence was not obtained with Klett–Fernald (β-AE~0). The α-AE profiles obtained from LIRIC retrievals also presented positive values (Figure 7f). The spectral dependence of the aerosol backscatter coefficient obtained with LIRIC was also observed in previous studies in cases of predominance of coarse particles. *Wagner et al.* [2013] suggested that this dependence might be caused by uncertainties of the spheroids model by AERONET, especially for scattering angles of 180°. On the other hand, this dependence is in full agreement with the employed microphysical model for describing the light scattering of nonspherical aerosol, and no superior model has been identified at present. As it was observed in the previous case, the aerosol backscatter coefficient is more dependent on the assumed model than the extinction profile due to the calculations of the lidar ratio.

The δ^P profile at 532 nm calculated from LIRIC output values were compared with those obtained from the lidar data using the approach described by *Bravo-Aranda et al.* [2013]. The δ^P values obtained from lidar data are around 17%, revealing the presence of mixed or aged mineral dust [*Freudenthaler et al.*, 2009]. Below 3 km asl, the δ^P decreased, indicating more contribution of anthropogenic or marine particles in agreement with the backward trajectory analysis performed with the HYSPLIT model. The δ^P retrieved from LIRIC outputs was also in this case a little bit lower (15%) above 2.5 km asl, although the discrepancies are within the uncertainty. Below 2.5 km asl, both δ^P profiles presented almost the same values, decreasing from 15 to 10%. Nevertheless, δ^P derived from LIRIC presents very constant values along the profile. The discrepancies between both approaches for computing δ^P can be explained in the same terms used in the previous case.

4.3. Case Study III: Mineral Dust, Smoke, and Pollution Cases on 10 September 2012

On 10 September 2012, a mixture of pollution, dust, and smoke was observed over Granada. HYSPLIT model (Figure S3b in the supporting information) indicated that the air masses came from the Mediterranean area in the lower part and from the Atlantic Ocean crossing over Africa at higher altitudes. The NAAPS

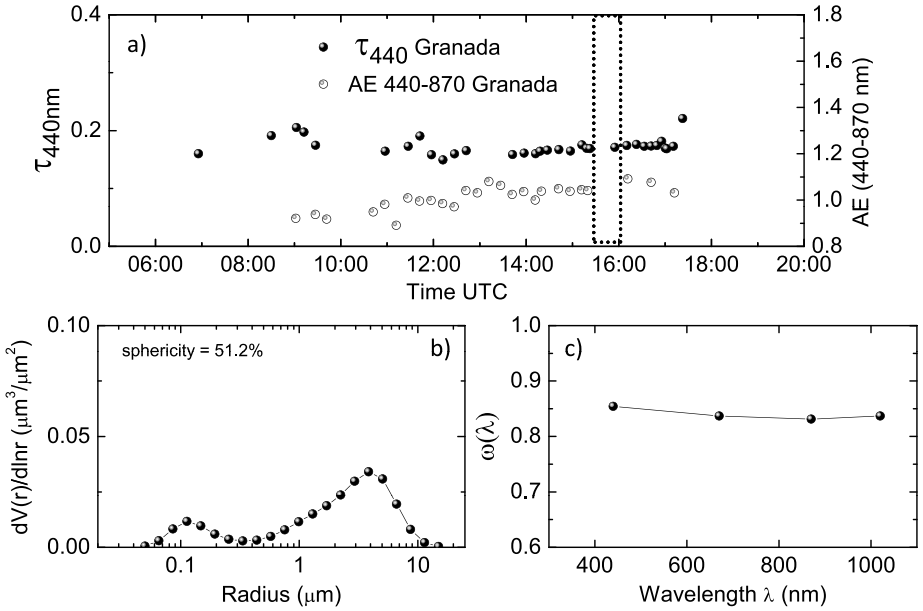

Figure 8. As in Figure 2 but for 10 September 2012. AERONET inversion data correspond to 15:56 UTC.

forecasting model (Figure S3c in the supporting information) indicated the presence of both sulphates and smoke over Europe and the Mediterranean basin and a slight presence of dust at Granada. Data obtained from the Web Fire Mapper of the FIRMS (Fire Information for Resource Management System, http://maps.geog.umd.edu/firms) [*Davies et al.*, 2009] (Figure S3d in the supporting information), indicate that several sources of active fires in North Africa and the southern Iberian Peninsula were close to the backward trajectories of the air masses arriving at Granada.

According to the AERONET data, the aerosol load was not very high over Granada, with τ_{440} values around 0.20 and almost constant along the day (Figure 8a). The values of AE(440–870 nm) were also very constant oscillating between 0.9 and 1.1. The aerosol fine fraction was 0.45, indicating a mixture of both fine and coarse particles. Size distribution retrieved at 15:56 UTC (Figure 8b) showed that the coarse mode almost doubled the fine one, presenting both rather low values. The $\omega(\lambda)$ values presented an almost neutral, slightly decreasing trend with λ and values around 0.85, suggesting the presence of a mixture of dust and smoke over Granada (Figure 8c) [*Dubovik et al.*, 2002].

Averaged lidar data between 15:30 and 16:00 UTC were combined with AERONET inversion at 15:56 UTC to retrieve the microphysical properties profiles. The initial set of user-defined input parameters is summarized in Table 1. Figure 9a shows the uncertainties obtained from the three different retrievals using the parameters from Table 1 but varying z_{N0}. (1175, 1385, and 1580 m asl). The highest uncertainties were obtained for the fine mode in the lower part of the profile (relative deviations around 25%). For the coarse spheroid mode, uncertainties were much lower, being maximum in the lower part of the profile with values around 5%. For the coarse spherical mode, the whole profile presented uncertainties around 1%.

In Figure 9b, the mean profiles and standard deviations were obtained from the three different retrievals with the input values from Table 1 but varying z_N between 3750 and 4150 m asl. The z_N variations in this case introduced very low uncertainties, lower than 1% in the whole profile for the three modes, as it occurred in the previous cases.

For this case, z_U values chosen for the three retrievals varied between 3900 and 4300 m asl. Variations in z_U introduced high uncertainties in the lower part of the profile, being around 20% for the fine mode, 5% for the coarse spherical mode, and below 1% for the coarse spheroid mode (Figure 9c). Fine and coarse spherical modes presented larger uncertainties when varying the upper limit due to the unrealistic offset introduced by the algorithm in the molecular height range for these two modes.

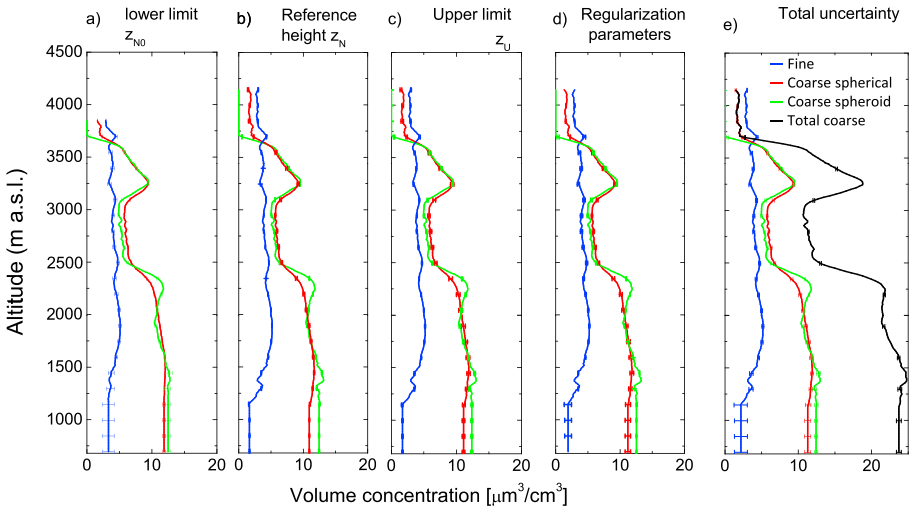

Figure 9. As in Figure 3 but for 10 September 2012. The total coarse mode profile (black line) in Figure 3e is retrieved without using the 532 nm cross-polarized channel from lidar data.

The regularization parameters were modified as in the two previous cases, obtaining five different retrievals corresponding to five different sets of values (Figure 9d). They introduced very low uncertainties for the three modes (lower than 2% in the whole profiles).

LIRIC mean volume concentration profiles obtained taking into account all the retrieved profiles with all possible variations are shown in Figure 9e. The largest uncertainties were obtained for the fine mode in the lower part of the profile with uncertainties around 20%. For the coarse spherical and coarse spheroid mode, uncertainties were much lower, with maximum values (~10%) also in the lower part of the profile.

For this case, the largest uncertainties were again caused by variations in the lower limit height z_{N0}. Very low uncertainties (below 2%) were obtained when varying the regularization parameters and the reference height. As in the pollution case, the largest deviations were obtained for the lower part of the profile.

There were mainly coarse particles of both modes (spherical and spheroids) with similar contribution. The sum of spherical and spheroid particles presented a very good agreement with the total coarse volume concentration profiles obtained without using the 532 nm cross-polarized channel, with differences lower than 4%. Maximum concentration values, reaching 12 $\mu m^3/cm^3$ for both the spherical and the spheroid modes, were obtained below 2500 m asl. Above this altitude, a maximum peak of 10 $\mu m^3/cm^3$ was observed around 3200 m asl. A slight and almost constant (~5 $\mu m^3/cm^3$) contribution of the fine mode was observed along the whole profile. Above 3750 m asl, the volume concentration was expected to be zero as indicated by the lidar elastic signals, but a positive offset was also clearly observed in this case for the fine and coarse spherical modes. This offset is larger for the fine mode, which is the one with the lowest volume concentration along the profile.

Figure 10 shows the comparison between optical properties profiles. In the case of the aerosol backscatter coefficient profiles, differences were larger for the infrared channel, whereas the agreement in the visible and ultraviolet was quite high. The lidar ratios profiles retrieved with LIRIC presented more similar values to the ones used in the Klett–Fernald method. For this case, negative values of the β-AE retrieved with LIRIC were obtained, especially in the part of the profile below 2500 m asl, where the ratio of coarse to fine particles is larger. However, the values of α-AE retrieved with LIRIC and that of β-AE retrieved with the Klett–Fernald method were positive and closer to the column integrated value provided by AERONET.

The δ^P profile, as in the two previous cases, was lower when obtained from LIRIC output data. Discrepancies in this case are quite remarkable, since δ^P obtained from the lidar data according to *Bravo-Aranda et al.* [2013] was twice the δ^P obtained from LIRIC retrievals. For both profiles, values were quite constant with height, being 5% according to LIRIC retrievals and over 10% according to lidar data.

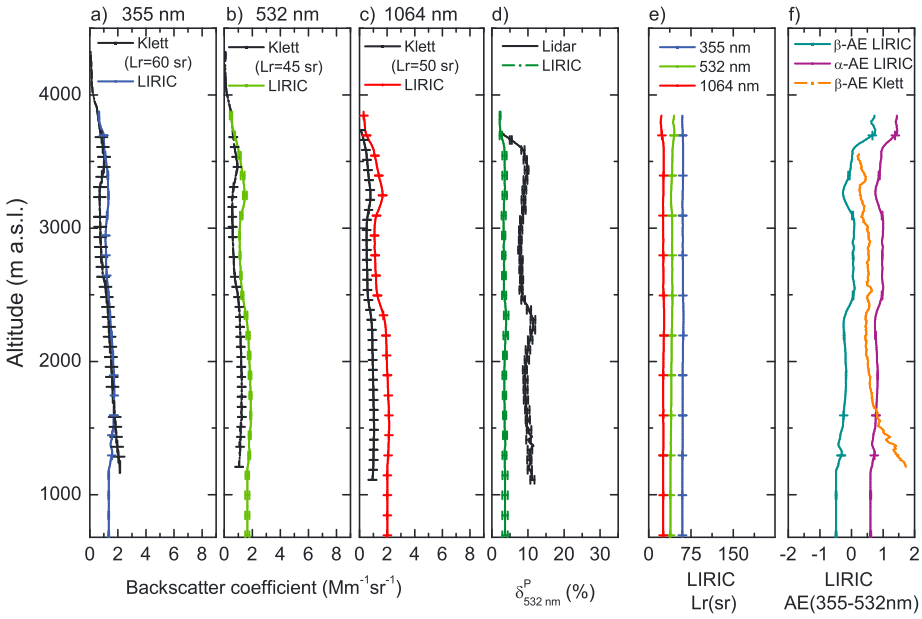

Figure 10. As in Figure 4 but for 10 September 2012.

5. Evaluation of LIRIC Performance Using Independent Sun Photometer Data at Two Altitude Levels

The use of the second Sun photometer in Cerro Poyos AERONET station allowed us to use the same lidar profiles to retrieve two different profiles of volume concentration, starting at different levels ($\Delta z = 1140$ m) in the same atmospheric column. This allows the possibility to check the coherence of both profiles over the upper station. This could be specially challenging when several layers of different aerosol types are present along the atmospheric column, since LIRIC assumes that properties such as the refractive index or the size distribution are height independent for each mode. Additionally, the retrievals using the second Sun photometer in Cerro Poyos station allows us to overcome the incomplete lidar overlap, avoiding the assumption of a constant volume concentration value below z_{N0} and in turn reducing the uncertainties.

5.1. Study Case IV: 30 July 2012

On 30 July 2012, another dust event occurred at Granada station. Five-day backward trajectories obtained with HYSPLIT model indicated that the air masses came from North Africa above 2 km asl. The Atlantic Ocean and the Iberian Peninsula were the source regions for the air masses at low altitudes (Figure S4b in the supporting information). BSC-DREAM8b and NAAPS models forecast the presence of mineral dust over the southeastern Iberian Peninsula, although the forecast loads were not very large (Figures S4c and S4d in the supporting information). For this date, data from the Sun photometer located at the mountain site in Cerro Poyos were available, so Figure 11 shows the AERONET data corresponding to both stations (Granada and Cerro Poyos). Data from the Sun photometer indicated that there was a high-aerosol load with τ_{440} increasing from 0.1 to 0.6 between 6:00 and 11:00 UTC. Low values of the AE(440–870 nm), below 0.20, especially after 09:00 UTC, indicated the predominance of coarse particles. Size distributions retrieved at 09:22 UTC showed a clear predominance of the coarse mode with quite high values at both altitudes. The $\omega(\lambda)$ had lower values over Granada, indicating that the layer between the surface and 1820 m asl had more absorbing particles than higher layers. The spectral dependence at both altitudes is typical of situations with mineral dust [*Dubovik et al.*, 2002; *Alados-Arboledas et al.*, 2008; *Valenzuela et al.*, 2012].

LIRIC volume concentration profiles were retrieved from lidar data between 10:00 and 10:30 UTC and the AERONET inversion at 09:22 UTC at both altitude levels (Figure 12).

Using AERONET data from Granada station and the user-defined input parameters in Table 2, the retrieved volume concentration profiles showed a clear predominance of the coarse spheroid mode, with values up to 80 $\mu m^3/cm^3$ and a slight contribution of the fine mode, reaching 10 $\mu m^3/cm^3$ from 3000 to 6600 m asl

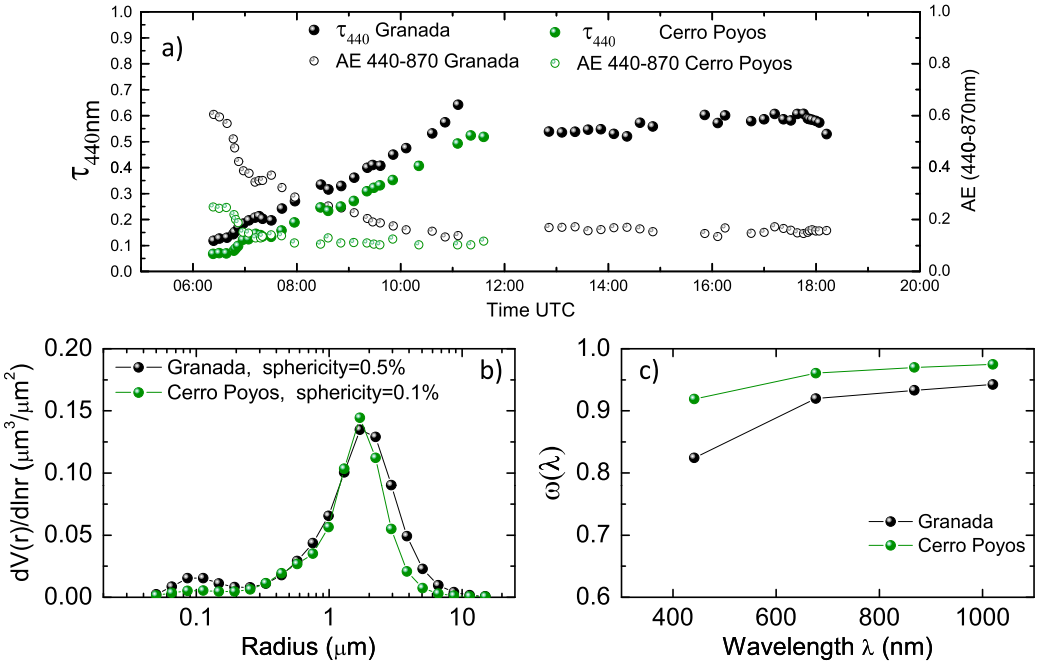

Figure 11. As in Figure 2 but for 30 July 2012. AERONET inversion data correspond to 09:22 UTC.

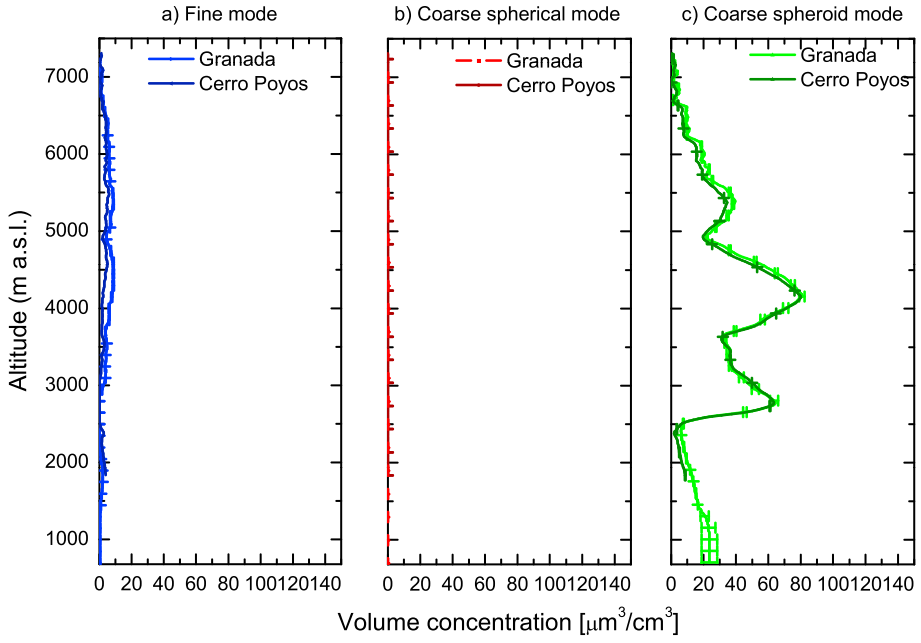

Figure 12. Volume concentration of the fine (a), coarse spherical (b), and coarse spheroid (c) modes for 30 July 2012 between 10:00 and 10:30 UTC with AERONET retrieval corresponding to 09:22 UTC from Granada station and lidar signals from 680 m asl and with AERONET retrieval corresponding to 09:22 UTC from Cerro Poyos station and lidar signals from 1820 m asl. Error bars indicate the standard deviations obtained by averaging the 12 retrievals described in section 3.2.

Table 2. As in Table 1 but for 30 July 2012 and 24 July 2012

Date	Case IV: 30 July 2012	Case V: 24 July 2012
z_{N0} (m asl)	1055	1080
z_N (m asl)	6860	3350
z_U (m asl)	7070	3500
k_{335}	$7.5 \cdot 10^{-4}$	$7.5 \cdot 10^{-4}$
k_{532}	$7.5 \cdot 10^{-4}$	$2.5 \cdot 10^{-4}$
k_{1064}	$2.5 \cdot 10^{-4}$	$2.5 \cdot 10^{-4}$
k_{532c}	$7.5 \cdot 10^{-5}$	$7.5 \cdot 10^{-5}$
f_{fine}	15	13
$f_{spherical}$	5	4
$f_{spheroid}$	10	12
d_{fine}	5	5
$d_{spherical}$	5	5
$d_{spheroid}$	5	5

(Figure 12). The coarse spheroid mode vertical profile retrieved by LIRIC presents three maximum values corresponding to the three different layers observed, with the largest concentrations around 4200 m asl, reaching the 80 $\mu m^3/cm^3$ value mentioned before. The error bars in Figure 12 were calculated as indicated in section 3.2.

The comparison between the profiles retrieved from Granada and Cerro Poyos is shown in Figure 12. The agreement for the coarse spheroid mode was high with differences below 5%. The coarse spherical mode was identical and practically null from both altitude levels. However, the fine mode presents larger values between 1820 and 3000 m asl when retrieved from Cerro Poyos, although differences are still very low (lower than 5 $\mu m^3/cm^3$). The good agreement between both retrievals is due to the strong contribution of the mineral dust along the whole atmospheric column above both altitude levels. So the assumption of a height independent aerosol model, based on height independent parameters for each mode such as the refractive index and the percentage of sphericity, did not introduce large uncertainties.

According to the results from section 3.2., variations in the lower limit value z_{N0} introduced the highest uncertainties in the performed tests. As the overlap do not affect the lidar signals from Cerro Poyos, z_{N0} is always set to 1820 m asl in LIRIC retrievals from this second AERONET station. This is the reason why error bars (computed as the standard deviations obtained by averaging the 12 retrievals described in section 3.3) are much lower when volume concentration profiles were retrieved from Cerro Poyos than when retrieved from Granada.

5.2. Study Case V: 24 July 2012

On 24 July 2012, a smoke plume was detected over Granada station according to lidar data (not shown). The combination of the 10 day backward trajectory analysis from HYSPLIT and MODIS FIRMS data indicated that the air masses advected smoke from North America, Portugal, and the northeast of the Iberian Peninsula and passed close to the North of Algeria, where some active fires were also observed (Figures S5b and S5d in the supporting information). The NAAPS model also forecast the presence of smoke over the Southeastern part of the Iberian Peninsula together with sulphates, indicating the presence of anthropogenic pollution.

AERONET data are shown in Figure 13. Time series show that aerosol optical properties were quite variable along the morning over Granada, with higher values of τ_{440} from 06:00 to 10:00 UTC. During this period, τ_{440} was much larger over Granada than over Cerro Poyos, where τ_{440} was almost constant around 0.20, indicating that the aerosol load was mainly below 1820 m asl. However, values were closer at both altitudes starting at midday. The AE(440–870 nm) values were smaller over Granada (~1.0) station than over Cerro Poyos (~1.4), which indicated a higher influence of the coarse mode below Cerro Poyos altitude level. AERONET inversion data were retrieved at the two altitudes at 15:22 UTC. At the time of the retrieval, 60% of the aerosol load was below Cerro Poyos. The size distributions showed very low values and very similar for both modes. Values for the coarse mode over Granada were higher than those over Cerro Poyos. The $\omega(\lambda)$ values above Granada were decreasing with wavelength, as it is usually observed for cases of biomass burning and anthropogenic pollution [*Dubovik et al.*, 2002]. However, it was higher above Cerro Poyos and almost wavelength independent. This behavior of the $\omega(\lambda)$ with wavelength can be explained by the aging processes suffered by the smoke, since it is affected by a long-range transport at altitudes over 4 km asl [*Eck et al.*, 2003].

For the retrieval with LIRIC, lidar data between 13:30 and 14:00 UTC and AERONET inversions at 15:22 UTC were used. LIRIC volume concentration profiles retrieved from Granada are shown in Figure 14. User-defined input parameters are in Table 2. There was a slight predominance of the coarse spherical mode in the whole profile, with maximum values in the layer between 2 and 3 km asl, reaching 20 $\mu m^3/cm^3$. Below 2.5 km,

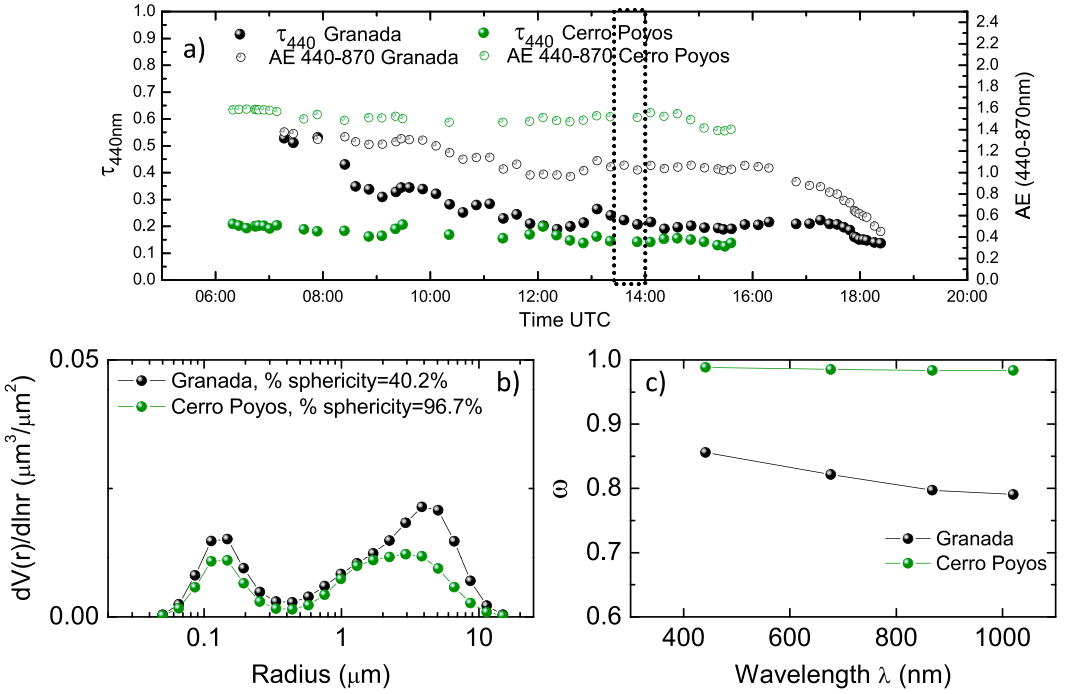

Figure 13. As in Figure 2 but for 24 July 2012.

the coarse spheroid mode was also considerable with volume concentration values of 10 $\mu m^3/cm^3$, but from this height, it was drastically reduced. The fine mode presented a small contribution (~5 $\mu m^3/cm^3$) up to 2 km asl and then increased having a maximum value of 15 $\mu m^3/cm^3$ around 2.9 km asl. Relative errors were below 25% for the fine mode and below 15% for coarse spheroid mode. For the coarse spherical mode relative errors were very low, being less than 10% except at the overlap region, reaching 15%.

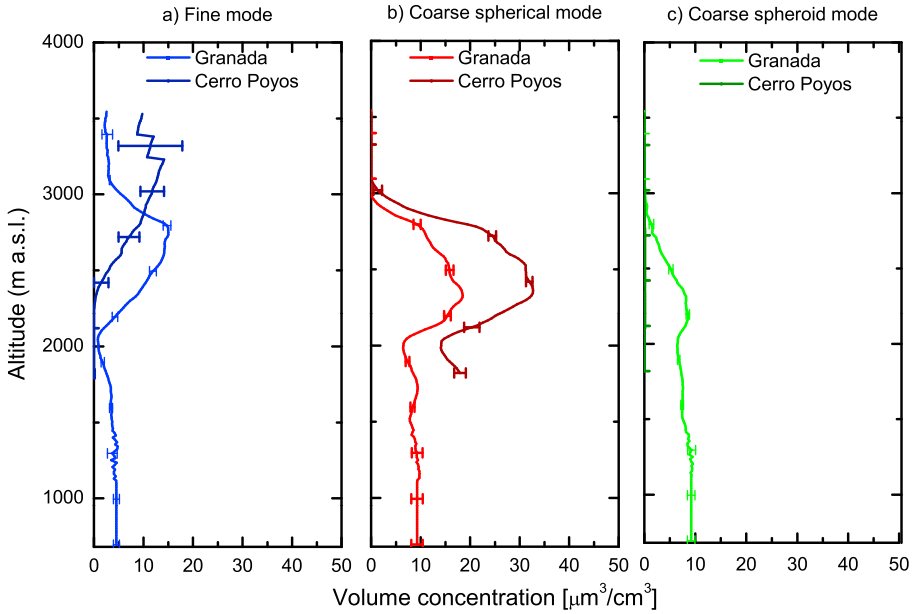

Figure 14. As in Figure 12 but for 24 July 2012.

Figure 14 also shows a direct comparison between the volume concentration profiles obtained from Granada and from Cerro Poyos stations. Some remarkable discrepancies were observed in this case. Coarse spheroid particles were not observed at all by the second Sun photometer at Cerro Poyos station, whereas according to the retrieval from Granada they reached almost 3 km asl. Maximum concentration of the coarse spherical mode was obtained at both altitude levels around 2.5 km asl, but values of the maximum were 18 and 33 $\mu m^3/cm^3$ for the retrievals from Granada and from Cerro Poyos, respectively. For the fine mode, similar values were obtained but the maximum was located much higher when data from Cerro Poyos station were used. The unrealistic offset introduced by LIRIC in the molecular region was affecting much more the fine mode in the retrieval from Cerro Poyos and variations in z_U values introduced large uncertainties, as it is observed in the error bars. For this specific situation, there was a good mixing in the lower part of the profile with very constant values of the aerosol optical properties and the assumption of constant volume concentrations below z_{N0} did not substantially affect the retrievals. Large discrepancies between the retrievals at both altitudes are partially caused by uncertainties of the measurements and by the spheroid model that drives AERONET aerosol retrievals and therefore LIRIC results too. In this sense, τ_{440} is quite low (~0.13) over Cerro Poyos being the retrieval accuracy of $\omega(\lambda)$ in the range 0.02–0.07 [*Dubovik et al.*, 2006]. Furthermore, it is necessary to take into account that the refractive index, percentage of sphericity and size distribution are assumed to be independent of the altitude when using LIRIC. According to the remote sensing data, for this case there were two layers of different aerosol types, so this assumption may introduce some important errors when using data from AERONET Granada station. Therefore, it is necessary to take into account these limitations of LIRIC under specific situations and quantify the uncertainties they can introduce in the retrievals.

6. Conclusions

LIRIC algorithm is evaluated and applied in this study. In a first part, three cases corresponding to three different atmospheric situations and different aerosol loadings and types have been analyzed using LIRIC. Several tests changing the different user-defined input parameters used in LIRIC software have been applied to these cases in order to determine the uncertainties and the consistency of the algorithm. In a second part of the study, two more study cases using data from a second Sun photometer located around 1 km above the lidar system have been used in order to obtain the microphysical properties profiles at two different altitudes using independent AERONET data to check the coherence of both profiles over the upper station.

LIRIC has proved to be a useful tool to retrieve vertical profiles of microphysical properties during daytime by combination of the lidar and the Sun photometer systems in a robust way. However intrinsic relative errors must be taken into account. Relative errors were maximum 33%, although they were usually below 15%. The parameter that induced more uncertainty was the lower limit z_{N0}, especially in those regions of the profiles closer to the surface. A possibility to reduce the uncertainty produced by this parameter could be the use of a near-field telescope to reduce the overlap of the lidar data. Also, the use of an overlap correction for the lidar data could reduce this uncertainty.

Uncertainties in the lower part of the profile, more affected by the algorithm assumption of a constant volume concentration value below the lower limit of the profile, were highly dependent on the vertical layering. In cases of good mixing within the boundary layer and low layering, the uncertainties were not very high (below 10%), but they reached higher values in cases of more complex structures (up to 30%). Uncertainties due to the regularization parameters and the reference height were usually very low, with values below 2%. Since the backscatter ratio at z_N is optimized by LIRIC algorithm in order to avoid the influence of aerosol backscatter in this molecular region, low uncertainties are obtained when varying this parameter (below 2%). However, for those cases when the reference height is located in a region with low signal-to-noise ratio uncertainties can reach even 17%.

An unrealistic offset introduced by the algorithm in the upper part of the profile was observed in the five cases presented here. This offset was more noticeable in those cases with low volume concentrations and especially in the modes with the lowest volume concentrations. The presence of this offset may be attributed to underestimations in the molecular extinction profiles, what may lead to an overestimation of the aerosol

volume concentration in the molecular region. The uncertainties introduced by changes in the upper limit z_U were highly dependent on this offset.

The comparison between optical properties profiles derived from LIRIC and those retrieved with Klett–Fernald showed that the best agreement is usually obtained for 532 nm. An unusual increase of the aerosol backscatter coefficient with wavelength was observed in the profiles retrieved by LIRIC in those cases with a predominance of the coarse mode. This unusual behavior is related to the use of AERONET microphysical model that drives the spectral behavior of the aerosol scattering. This model assumes nonspherical particles as spheroids that are a simplified shape. This assumption may introduce some uncertainties especially at the scattering angle $\theta = 180°$. On the other hand the phase function of mixture of dust particles of any shape always has some spectral dependence and therefore, the observed spectral feature might be real. This needs to be verified in future studies. However, the aerosol extinction coefficient is not sensitive to the particle shape assumption, and no anomalies were observed for this property.

The δ^P profiles retrieved from LIRIC output results, and those retrieved from lidar data presented important discrepancies. In general, larger values were obtained from the lidar data. This can be explained by the fact that it is necessary to take into account the polarizing effects associated to the different optical and the misalignment between the polarization plane of the laser and the optical devices. Excluding the cross talk between 532-cross and 532-parallel channels, these effects are not considered in LIRIC.

The comparison between the retrieved volume concentration profiles above Granada and above Cerro Poyos, using independent AERONET data at two altitudes but in the same atmospheric column, indicated that the method is quite robust. The agreement between the profiles retrieved using data from the two different stations is very good, with differences below 10% in those cases with the same type of aerosol and the most part of the aerosol load over both stations. However, the assumption of height independent values of the lidar ratio, the size distribution, and refractive index may introduce large uncertainties in LIRIC retrievals in those cases with different types of aerosol at different heights. GARRLIC algorithm may reduce these errors since more vertical information from the lidar system is taken into account.

Acknowledgments

This work was supported by the Spanish Ministry of Science and Technology through projects CGL2008-01330-E/CLI (Spanish and Portuguese Lidar Network), CGL2010-18782, and CSD2007-00067; by the Andalusian Regional Government through projects P10-RNM-6299 and P12-RNM-2409 and by EU through ACTRIS project (EU INFRA-2010-1.1.16-262254). Granados-Muñoz was funded under grant AP2009-0552. The authors thankfully acknowledge the computer resources, technical expertise, and assistance provided by the Barcelona Supercomputing Center for the BSC-DREAM8b model dust data. The authors express gratitude to the NOAA Air Resources Laboratory for the HYSPLIT transport and dispersion model. We also thank those at the NRL-Monterey that helped in the development of the NAAPS model and to the MODIS team for the use of FIRMS data. Finally, the authors thank to Sierra Nevada National Park for the support in the maintenance of the Sun photometer station at Cerro Poyos.

References

Alados-Arboledas, L., A. Alcántara, F. J. Olmo, J. A. Martínez-Lozano, V. Estellés, V. Cachorro, A. M. Silva, H. Horvath, M. Gangl, and A. Díaz (2008), Aerosol columnar properties retrieved from CIMEL radiometers during VELETA 2002, *Atmos. Environ.*, *42*(11), 2654–2667.

Alados-Arboledas, L., D. Müller, J. L. Guerrero-Rascado, F. Navas-Guzmán, D. Pérez-Ramírez, and F. J. Olmo (2011), Optical and microphysical properties of fresh biomass burning aerosol retrieved by Raman lidar, and star-and sun-photometry, *Geophys. Res. Lett.*, *38*, L01807, doi:10.1029/2010GL045999.

Amiridis, V., D. S. Balis, S. Kazadzis, A. Bais, E. Giannakaki, A. Papayannis, and C. Zerefos (2005), Four-year aerosol observations with a Raman lidar at Thessaloniki, Greece, in the framework of European Aerosol Research Lidar Network (EARLINET), *J. Geophys. Res.*, *110*, D21203, doi:10.1029/2005JD006190.

Ansmann, A., U. Wandinger, M. Riebesell, C. Weitkamp, and W. Michaelis (1992), Independent measurement of extinction and backscatter profiles in cirrus clouds by using a combined Raman elastic-backscatter lidar, *Appl. Opt.*, *31*(33), 7113.

Ansmann, A., F. Wagner, D. Müller, D. Althausen, A. Herber, W. von Hoyningen-Huene, and U. Wandinger (2002), European pollution outbreaks during ACE 2: Optical particle properties inferred from multiwavelength lidar and star-Sun photometry, *J. Geophys. Res.*, *107*(D15), 4259, doi:10.1029/2001JD001109.

Barnaba, F., and G. P. Gobbi (2004), Aerosol seasonal variability over the Mediterranean region and relative impact of maritime, continental and Saharan dust particles over the basin from MODIS data in the year 2001, *Atmos. Chem. Phys.*, *4*(9/10), 2367–2391.

Böckmann, C., I. Mironova, D. Müller, L. Schneidenbach, and R. Nessler (2005), Microphysical aerosol parameters from multiwavelength lidar, *J. Opt. Soc. Am. A Opt. Image Sci.*, *22*(3), 518–528.

Bösenberg, J., et al. (2001), EARLINET: Establishing the European Aerosol Research Lidar Network, in *Lidar Remote Sensing in Atmospheric and Earth Sciences, Proceedings of the 21st International Laser Radar Conference*, edited by L. Bissonette, G. Roy, and G. Vallèe, Defense R&D Canada–Valcartier, Val-Belair, Quebec, Canada, 293, 2002.

Boucher, O., et al. (2013), Clouds and Aerosols, in *Climate Change 2013: The Physical Science Basis. Contribution of Working Group I to the Fifth Assessment Report of the Intergovernmental Panel on Climate Change*, edited by T. F. Stocker et al., Cambridge Univ. Press, Cambridge, U. K., and New York.

Bravo-Aranda, J. A., F. Navas-Guzmán, J. L. Guerrero-Rascado, D. Pérez-Ramírez, M. J. Granados-Muñoz, and L. Alados-Arboledas (2013), Analysis of lidar depolarization calibration procedure and application to the atmospheric aerosol characterization, *Int. J. Remote Sens.*, *34*(9–10), 3543–3560.

Chaikovsky, A., O. Dubovik, P. Goloub, N. Balashevich, A. Lopatsin, Y. Karol, S. Denisov, and T. Lapyonok (2008), Software package for the retrieval of aerosol microphysical properties in the vertical column using combined lidar/photometer data (test version), *Tech. Rep.*, Institute of Physics, National Academy of Sciences of Belarus, Minsk, Belarus.

Chaikovsky, A., et al. (2012), Algorithm and software for the retrieval of vertical aerosol properties using combined lidar/radiometer data: Dissemination in EARLINET, paper presented at 26th International Laser and Radar Conference, Porto Heli, Greece.

Christensen, J. H. (1997), The Danish Eulerian hemispheric model—A three-dimensional air pollution model used for the Arctic, *Atmos. Environ.*, *31*(24), 4169–4191.

Cuesta, J., P. H. Flamant, and C. Flamant (2008), Synergetic technique combining elastic backscatter lidar data and sunphotometer AERONET inversion for retrieval by layer of aerosol optical and microphysical properties, *Appl. Opt.*, *47*(25), 4598–4611.
Davies, D. K., S. Ilavajhala, M. M. Wong, and C. O. Justice (2009), Fire information for resource management system: Archiving and distributing MODIS active fire data, *IEEE Trans. Geosci. Remote Sens.*, *47*(1), 72–79.
Draxler, R. R., and G. D. Rolph (2003), HYSPLIT (HYbrid Single-Particle Lagrangian Integrated Trajectory) model, NOAA Air Resources Laboratory, Silver Spring, Md. [Access via NOAA ARL READY website, http://www.arl.noaa.gov/ready/hysplit4.html.]
Dubovik, O., and M. D. King (2000), A flexible inversion algorithm for retrieval of aerosol optical properties from Sun and sky radiance measurements, *J. Geophys. Res.*, *105*, 20,673–20,696, doi:10.1029/2000JD900282.
Dubovik, O., B. Holben, T. F. Eck, A. Smirnov, Y. J. Kaufman, M. D. King, D. Tanré, and I. Slutsker (2002), Variability of absorption and optical properties of key aerosol types observed in worldwide locations, *J. Atmos. Sci.*, *59*(3), 590–608.
Dubovik, O., et al. (2006), Application of spheroid models to account for aerosol particle nonsphericity in remote sensing of desert dust, *J. Geophys. Res.*, *111*, D11208, doi:10.1029/2005JD006619.
Eck, T. F., B. N. Holben, J. S. Reid, O. Dubovik, A. Smirnov, N. T. O'Neill, I. Slutsker, and S. Kinne (1999), Wavelength dependence of the optical depth of biomass burning, urban, and desert dust aerosols, *J. Geophys. Res.*, *104*, 31,333–31,349, doi:10.1029/1999JD900923.
Eck, T. F., B. N. Holben, J. S. Reid, N. T. O'Neill, J. S. Schafer, O. Dubovik, A. Smirnov, M. A. Yamasoe, and P. Artaxo (2003), High aerosol optical depth biomass burning events: A comparison of optical properties for different source regions, *Geophys. Res. Lett.*, *30*(20), 2035, doi:10.1029/2003GL017861.
Estellés, V., et al. (2006), Intercomparison of spectroradiometers and Sun photometers for the determination of the aerosol optical depth during the VELETA-2002 field campaign, *J. Geophys. Res.*, *111*, D17207, doi:10.1029/2005JD006047.
Fernald, F. G. (1984), Analysis of atmospheric lidar observations- Some comments, *Appl. Opt.*, *23*(5), 652–653.
Fernald, F. G., B. M. Herman, and J. A. Reagan (1972), Determination of aerosol height distributions by lidar, *J. Appl. Meteorol.*, *11*(3), 482–489.
Forster, P., et al. (2007), Changes in Atmospheric Constituents and in Radiative Forcing, in *Climate Change 2007: The Physical Science Basis. Contribution of Working Group I to the Fourth Assessment Report of the Intergovernmental Panel on Climate Change*, edited by S. Solomon et al., Cambridge Univ. Press, Cambridge, U. K., and New York.
Franke, K., A. Ansmann, D. Müller, D. Althausen, F. Wagner, and R. Scheele (2001), One-year observations of particle lidar ratio over the tropical Indian Ocean with Raman lidar, *Geophys. Res. Lett.*, *28*, 4559–4562, doi:10.1029/2001GL013671.
Freudenthaler, V., M. Esselborn, M. Wiegner, B. Heese, M. Tesche, A. Ansmann, D. Müller, D. Althausen, M. Wirth, and A. Fix (2009), Depolarization ratio profiling at several wavelengths in pure Saharan dust during SAMUM 2006, *Tellus, Ser. B*, *61*(1), 165–179.
Grams, G. W., I. H. Blifford Jr., B. G. Schuster, and J. S. DeLuisi (1972), Complex index of refraction of airborne fly ash determined by laser radar and collection of particles at 13 km, *J. Atmos. Sci.*, *29*, 900–905.
Guerrero-Rascado, J. L., B. Ruiz, and L. Alados-Arboledas (2008), Multi-spectral Lidar characterization of the vertical structure of Saharan dust aerosol over southern Spain, *Atmos. Environ.*, *42*(11), 2668–2681.
Guerrero-Rascado, J. L., F. J. Olmo, I. Avilés-Rodríguez, F. Navas-Guzmán, D. Pérez-Ramírez, H. Lyamani, and L. Alados-Arboledas (2009), Extreme Saharan dust event over the southern Iberian Peninsula in September 2007: Active and passive remote sensing from surface and satellite, *Atmos. Chem. Phys.*, *9*(21), 8453–8469.
Guerrero-Rascado, J. L., et al. (2011), Aerosol closure study by lidar, Sun photometry, and airborne optical counters during DAMOCLES field campaign at El Arenosillo sounding station, Spain, *J. Geophys. Res.*, *116*, D02209, doi:10.1029/2010JD014510.
Holben, B. N., et al. (1998), AERONET—A federated instrument network and data archive for aerosol characterization, *Remote Sens. Environ.*, *66*(1), 1–16.
Kaufman, Y. J., D. Tanré, J. F. Léon, and J. Pelon (2003), Retrievals of profiles of fine and coarse aerosols using lidar and radiometric space measurements, *IEEE Trans. Geosci. Remote Sens.*, *41*(8), 1743–1754.
Klett, J. D. (1981), Stable analytical inversion solution for processing lidar returns, *Appl. Opt.*, *20*(2), 211–220.
Klett, J. D. (1985), Lidar inversion with variable backscatter/extinction ratios, *Appl. Opt.*, *24*(11), 1638–1643.
Kokkalis, P., A. Papayannis, V. Amiridis, R. E. Mamouri, I. Veselovskii, A. Kolgotin, G. Tsaknakis, N. I. Kristiansen, A. Stohl, and L. Mona (2013), Optical, microphysical, mass and geometrical properties of aged volcanic particles observed over Athens, Greece, during the Eyjafjallajökull eruption in April 2010 through synergy of Raman lidar and sunphotometer measurements, *Atmos. Chem. Phys.*, *13*, 9303–9320.
Léon, J.-F., D. Tanré, J. Pelon, Y. J. Kaufman, J. M. Haywood, and B. Chatenet (2003), Profiling of a Saharan dust outbreak based on a synergy between active and passive remote sensing, *J. Geophys. Res.*, *108*(D18), 8575, doi:10.1029/2002JD002774.
Lopatin, A., O. Dubovik, A. Chaikovsky, P. Goloub, T. Lapyonok, D. Tanré, and P. Litvinov (2013), Enhancement of aerosol characterization using synergy of lidar and sun-photometer coincident observations: The GARRLiC algorithm, *Atmos. Meas. Tech.*, *6*, 2253–2325.
Lyamani, H., F. J. Olmo, and L. Alados-Arboledas (2005), Saharan dust outbreak over southeastern Spain as detected by sun photometer, *Atmos. Environ.*, *39*(38), 7276–7284.
Lyamani, H., F. J. Olmo, A. Alcántara, and L. Alados-Arboledas (2006a), Atmospheric aerosols during the 2003 heat wave in southeastern Spain I: Spectral optical depth, *Atmos. Environ.*, *40*(33), 6453–6464.
Lyamani, H., F. J. Olmo, A. Alcántara, and L. Alados-Arboledas (2006b), Atmospheric aerosols during the 2003 heat wave in southeastern Spain II: Microphysical columnar properties and radiative forcing, *Atmos. Environ.*, *40*(33), 6465–6476.
Mattis, I., A. Ansmann, D. Müller, U. Wandinger, and D. Althausen (2004), Multiyear aerosol observations with dual-wavelength Raman lidar in the framework of EARLINET, *J. Geophys. Res.*, *109*, D13203, doi:10.1029/2004JD004600.
Müller, D., U. Wandinger, and A. Ansmann (1999), Microphysical particle parameters from extinction and backscatter lidar data by inversion with regularization: Theory, *Appl. Opt.*, *38*(12), 2346–2357.
Müller, D., A. Ansmann, I. Mattis, M. Tesche, U. Wandinger, D. Althausen, and G. Pisani (2007), Aerosol-type-dependent lidar ratios observed with Raman lidar, *J. Geophys. Res.*, *112*, D16202, doi:10.1029/2006JD008292.
Müller, D., I. Veselovskii, A. Kolgotin, M. Tesche, A. Ansmann, and O. Dubovik (2013), Vertical profiles of pure dust and mixed smoke–dust plumes inferred from inversion of multiwavelength Raman/polarization lidar data and comparison to AERONET retrievals and in situ observations, *Appl. Opt.*, *52*(14), 3178–3202.
Navas-Guzmán, F., J. L. G. Rascado, and L. A. Arboledas (2011), Retrieval of the lidar overlap function using Raman signals, *Opt. Pura Apl.*, *44*(1), 71–75.
Navas-Guzmán, F., D. Müller, J. A. Bravo-Aranda, J. L. Guerrero-Rascado, M. J. Granados-Muñoz, D. Pérez-Ramírez, F. J. Olmo, and L. Alados-Arboledas (2013a), Eruption of the Eyjafjallajökull Volcano in spring 2010: Multiwavelength Raman lidar measurements of sulphate particles in the lower troposphere, *J. Geophys. Res. Atmos.*, *118*, 1804–1813, doi:10.1002/jgrd.50116.
Navas-Guzmán, F., J. A. Bravo-Aranda, J. L. Guerrero-Rascado, M. J. Granados-Muñoz, and L. Alados-Arboledas (2013b), Statistical analysis of aerosol optical properties retrieved by Raman lidar over Southeastern Spain, *Tellus, Ser. B*, *65*, 21,234.

Pappalardo, G., et al. (2004), Aerosol lidar intercomparison in the framework of the EARLINET project. 3. Raman lidar algorithm for aerosol extinction, backscatter, and lidar ratio, *Appl. Opt.*, *43*, 5370–5385.

Pérez-Ramírez, D., F. Navas-Guzmán, H. Lyamani, J. Fernández-Gálvez, F. J. Olmo, and L. Alados-Arboledas (2012), Retrievals of precipitable water vapor using star photometry: Assessment with Raman lidar and link to sun photometry, *J. Geophys. Res.*, *117*, D05202, doi:10.1029/2011JD016450.

Preißler, J., F. Wagner, J. L. Guerrero-Rascado, and A. M. Silva (2013), Two years of free-tropospheric aerosol layers observed over Portugal by lidar, *J. Geophys. Res. Atmos.*, *118*, 3676–3686, doi:10.1002/jgrd.50350.

Reagan, J. A., J. D. Spinhirne, D. M. Byrne, D. W. Thomson, R. G. De Pena, and Y. Mamane (1977), Atmospheric particulate properties inferred from lidar and solar radiometer observations compared with simultaneous in situ aircraft measurements: A case study, *J. Appl. Meteorol.*, *16*, 911–928.

Sasano, Y., E. V. Browell, and S. Ismail (1985), Error caused by using a constant extinction/backscattering ratio in the lidar solution, *Appl. Opt.*, *24*(22), 3929–3932.

Uthe, E. E. (1982), Particle size evaluations using multiwavelength extinction measurements, *Appl. Opt.*, *21*(3), 454–459.

Valenzuela, A., F. J. Olmo, H. Lyamani, M. Antón, A. Quirantes, and L. Alados-Arboledas (2012), Classification of aerosol radiative properties during African desert dust intrusions over southeastern Spain by sector origins and cluster analysis, *J. Geophys. Res.*, *117*, D06214, doi:10.1029/2011JD016885.

Veselovskii, I., A. Kolgotin, V. Griaznov, D. Müller, U. Wandinger, and D. N. Whiteman (2002), Inversion with regularization for the retrieval of tropospheric aerosol parameters from multiwavelength lidar sounding, *Appl. Opt.*, *41*(18), 3685–3699.

Veselovskii, I., O. Dubovik, A. Kolgotin, T. Lapyonok, P. Di Girolamo, D. Summa, D. N. Whiteman, M. Mishchenko, and D. Tanré (2010), Application of randomly oriented spheroids for retrieval of dust particle parameters from multiwavelength lidar measurements, *J. Geophys. Res.*, *115*, D21203, doi:10.1029/2010JD014139.

Wagner, J., A. Ansmann, U. Wandinger, P. Seifert, A. Schwarz, M. Tesche, A. Chaikovsky, and O. Dubovik (2013), Evaluation of the Lidar/Radiometer Inversion Code (LIRIC) to determine microphysical properties of volcanic and desert dust, *Atmos. Meas. Tech.*, *6*(7), 1707–1724.

Wandinger, U., A. Ansmann, J. Reichardt, and T. Deshler (1995), Determination of stratospheric aerosol microphysical properties from independent extinction and backscattering measurements with a Raman lidar, *Appl. Opt.*, *34*(36), 8315–8329.

Wiegner, M., and A. Geiß (2012), Aerosol profiling with the JenOptik ceilometer CHM15kx, *Atmos. Meas. Tech.*, *5*(3), 3395–3430.